

## REVIEW

View Article Online  
View Journal | View IssueCite this: *Org. Chem. Front.*, 2021, **8**, 7050Received 2nd August 2021,  
Accepted 5th October 2021

DOI: 10.1039/d1qo01139a

rsc.li/frontiers-organic

# Metal-hydride hydrogen atom transfer (MHAT) reactions in natural product synthesis

Jinghua Wu and Zhiqiang Ma \*

The metal-hydride hydrogen atom transfer (MHAT) reaction plays an important role in the field of natural product synthesis. MHAT, as a powerful method, has been employed by chemists to construct C–C, C–H, and C–heteroatom bonds. In this review, we summarize the recent total synthesis of natural products using MHAT to functionalize olefins with first-row transition metal catalysts such as cobalt, manganese and iron.

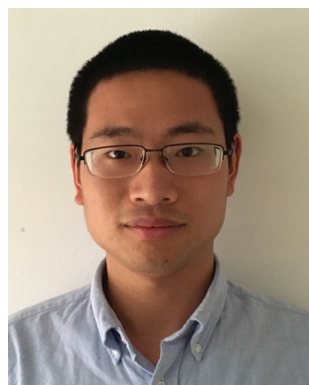
## 1. Introduction

Functionalization of olefins has been an important transformation in synthetic chemistry. In particular, functionalization of unactivated olefins is a difficult task. The metal-hydride hydrogen atom transfer (MHAT) reaction plays an important role in functionalization of olefins.

In 1979, Tabushi achieved the hydration of cyclohexene under Mn-catalyzed conditions employing NaBH<sub>4</sub> and air.<sup>1</sup> In 1989, Mukaiyama reported Co-catalyzed hydration of olefins utilizing alcohol as the solvent and reductant,<sup>2</sup> and he sub-

sequently used silicon hydride as the hydrogen source instead of alcohols.<sup>3</sup> In the following decades, the hydride atom transfer reaction using silicon hydride as the hydrogen source has been greatly developed, and diverse types of MHAT reactions have been reported. Researchers including Carreira,<sup>4</sup> Shenvi,<sup>5</sup> Herzon,<sup>6</sup> Baran,<sup>7</sup> and Boger<sup>8</sup> and many others expanded the MHAT reaction. They reported the construction of carbon–carbon, carbon–heteroatom and carbon–hydrogen bonds from olefins, based on the generation of carbon-centered radicals. In light of the development, the application of MHAT reactions in total synthesis of natural products is booming, especially in recent years. In 2016 and 2018, Shenvi reviewed the development of metal-hydride hydrogen atom transfer reactions.<sup>9</sup> There were also some related reviews disclosed afterward.<sup>10</sup> This review focuses on the natural product synthesis employing the MHAT reaction as the key strategy, and basically covers

Key Lab of Functional Molecular Engineering of Guangdong Province, School of Chemistry & Chemical Engineering, South China University of Technology, Wushan Road-381, Guangzhou 510641, People's Republic of China.  
E-mail: cezqma@scut.edu.cn



Jinghua Wu

Jinghua Wu was born in Fujian, China. He received his B.Sc. from Beijing University of Chemical Technology in 2016. Currently, Jinghua Wu is a graduate student in the group of Professor Zhiqiang Ma at South China University of Technology, where he focuses on natural product synthesis.



Zhiqiang Ma

Zhiqiang Ma obtained his BS in chemistry from Lanzhou University in 2001, and PhD in organic chemistry from Shanghai Institute of Organic Chemistry, Chinese Academy of Sciences with Professor Hongbin Zhai in 2007. In the same year, he joined Prof. Chuo Chen's group at UT Southwestern Medical Center as a postdoctoral fellow. Since then, he has been working on the total synthesis of pyrrole-imidazole natural products.

Currently, he is a faculty member in South China University of Technology. His research interests focus on natural product synthesis, target-oriented methodology development and medicinal chemistry.

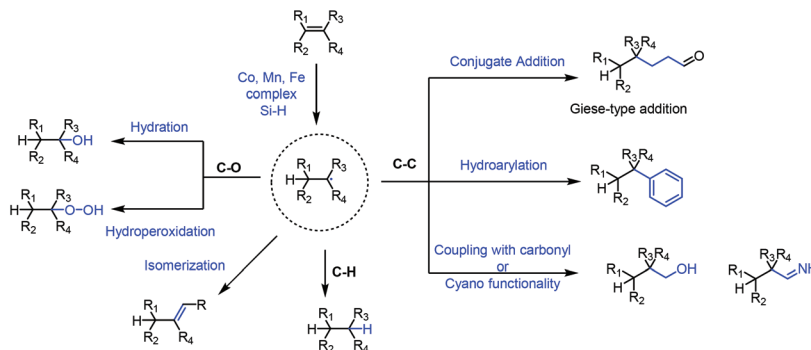


Fig. 1 MHAT-based reactions of olefins.

the examples reported after 2016. We have basically divided the review into four sections based on the type of bond formation, including C–C, C–O, and C–H bonds, and isomerization as shown in Fig. 1. We will summarize the construction of C–C bonds from olefins through MHAT first, including conjugate addition, hydroarylation, and addition to carbonyl or cyano groups. Next, hydration and hydroperoxidation of olefins are discussed. Hydrogenation of olefins and isomerization are discussed last.

## 2. C–C bond formation

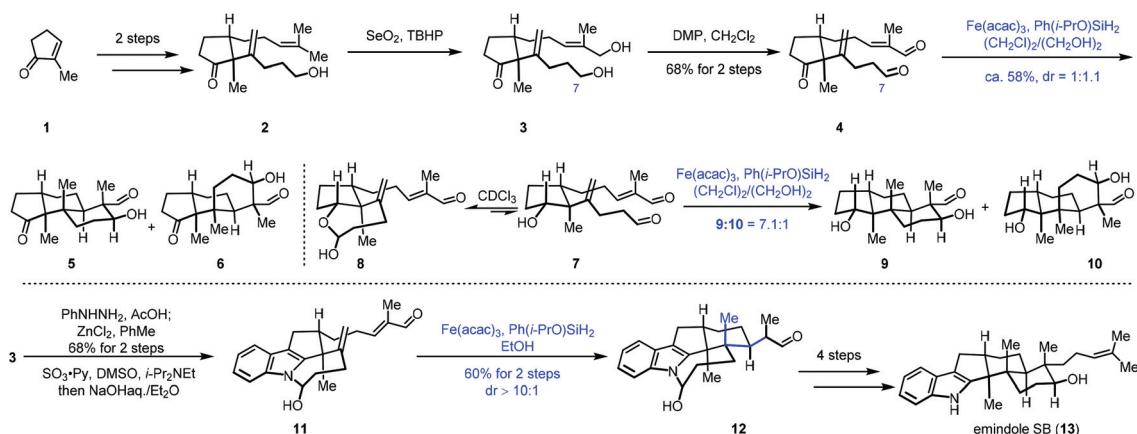
Based on the proposed mechanism of the MHAT reaction, carbon-centered radicals would be formed from olefins *via* MHAT, and diverse types of reactions, such as conjugate addition, hydroarylation, and addition to carbonyl or cyano groups, occur when different radical acceptors are present.

### 2.1 Conjugate addition

Addition of nucleophilic radicals to electron-deficient olefins is called the Giese reaction,<sup>11</sup> which is a useful approach for C–C bond construction. In 2010, Ishibashi reported iron-catalyzed radical cyclization of 1,6-dienes.<sup>12</sup> Subsequently in 2014,

Baran developed cross-coupling of unactivated olefins and electron-deficient olefins under mild conditions with Fe(acac)<sub>3</sub> or Fe(dibm)<sub>3</sub> as catalysts and PhSiH<sub>3</sub> as the hydrogen source. Baran's work has greatly expanded the application of MHAT in the construction of C–C bonds. They further realized the cross-coupling reaction of heteroatom-substituted olefins with electron-deficient olefins.<sup>7</sup>

This powerful method was utilized by Pronin to accomplish the synthesis of emindole SB (**13**).<sup>13</sup> In 2015, Pronin and co-workers employed iron-catalyzed intramolecular conjugate addition and aldol reaction to achieve polycyclization (Scheme 1). Their synthesis commenced with the cyclopentanone derivative **1**, which was transformed to **2** *via* a two-step sequence. Continuous oxidation gave **4**. The authors then tried to achieve polycyclization of **4** to establish the tricyclic core of emindole SB (**13**) *via* Fe-catalyzed HAT reaction. Under the conditions (Fe(acac)<sub>3</sub>, Ph(*i*-PrO)SiH<sub>2</sub>, (CH<sub>2</sub>Cl)<sub>2</sub>, and EtOH), the polycyclization occurred through conjugate addition and aldol reaction, giving tricyclic core products **5** and **6** with a 1 : 1.1 dr. The authors found that the C7 aldehyde of **4** existed predominantly in its hemiacetal form in alcoholic solvents, and then they proposed that reversible cyclic hemiacetal intermediates would be formed when a hydroxyl group instead of a ketone group is present in the precursor. Indeed, substrate **7** existed



Scheme 1 Pronin's synthesis of emindole SB (**13**).

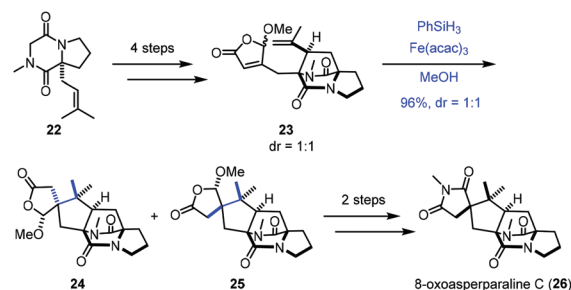
as a 1:2 mixture with the corresponding cyclic hemiacetal **8**. The authors envisioned that the cyclic hemiacetal of **8** could allow for the desired stereocontrol over the initial radical cyclization. As expected, exposure of **7** to similar polycyclization conditions with lower temperature delivered a mixture of **9** and **10** with a 7.1:1 dr, favoring the desired scaffold **9**. Accordingly, the authors speculated that the hemiaminal intermediate resulting from an indole N–H could induce similar stereoselective cyclization. A Fischer indole synthesis from **3** followed by oxidation furnished a dialdehyde, which was transformed to hemiaminal **11** in the presence of NaOH. Upon exposure of hemiaminal **11** to the conditions of Fe(acac)<sub>3</sub> and Ph(*i*-PrO)SiH<sub>2</sub>, conjugate addition occurred, providing the pentacyclic intermediate **12** in 60% yield over two steps. In this conversion, three stereocenters were established with excellent selectivity. Lastly, a four-step sequence was performed to give emindole SB (**13**).

In 2017, Maimone and co-workers achieved the syntheses of andrastin D (**17**), preterrenoid (**19**), terrenoid (**20**), and terretinin L (**21**) (Scheme 2).<sup>14</sup> Their syntheses started with **14**, an intermediate in the synthesis of berkeleyone A.<sup>15</sup> **14** could be oxidized to **15** with PCC, which was further converted into **16** *via* a rearrangement reaction with the intermediacy of carbocations that were generated by the modified Shigehisa conditions (cat. Co-1, PhSiH<sub>3</sub>, and **F1**).<sup>16</sup> The authors observed that increasing the equivalents of **F1** and PhSiH<sub>3</sub> from 1.0 to 2.5 could furnish **16** in 90% yield. The authors also tested a variety of Brønsted acids, and it turned out that these acidic conditions failed to induce the expected rearrangement. With **16** in hand, a Krapcho-type demethylation provided andrastin D (**17**). In 2008, Carreira reported the hydrochlorination of unactivated olefins under Co-catalyzed HAT in the presence of *para*-toluenesulfonyl chloride (TsCl).<sup>4f</sup> Compared to conventional hydrochlorination reactions, Carreira's method has good functional group compatibility. Under Carreira's conditions,<sup>4f</sup> Maimone and co-workers observed that a terretinin

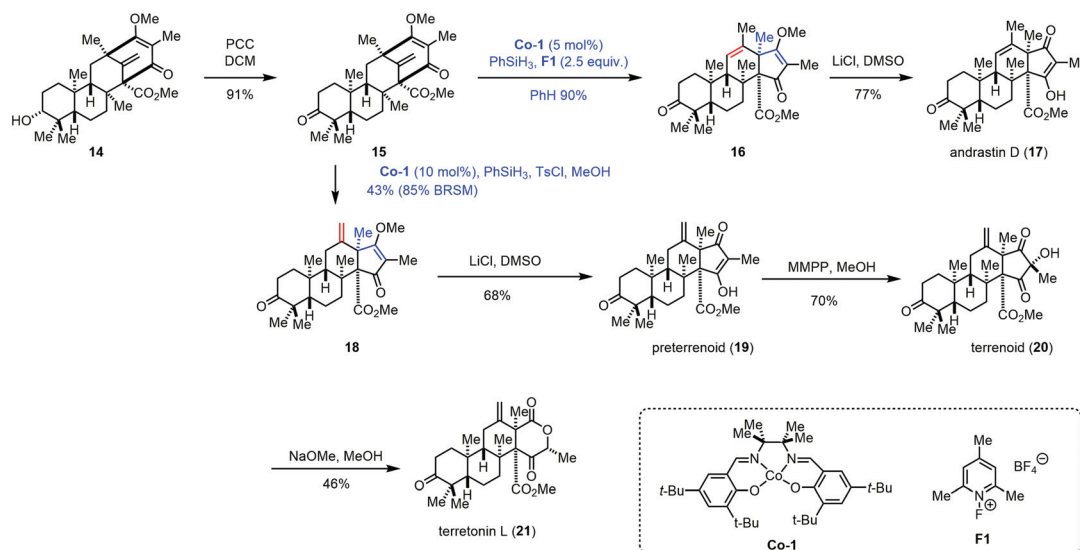
core skeleton (**18**) could be formed preferentially from **15**, which was then advanced to preterrenoid (**19**), terrenoid (**20**), and terretinin L (**21**).

In 2017, Jahn employed Baran's reductive radical cyclizations to achieve the synthesis of 8-oxoasperparaline C (**26**) (Scheme 3).<sup>17</sup> In the event,  $\gamma$ -methoxybutenolide **23** was prepared from **22** *via* a four-step sequence. Treatment of **23** with Fe(acac)<sub>3</sub> and PhSiH<sub>3</sub> generated the corresponding tertiary radical, which underwent Giese-type radical conjugate addition with an unsaturated  $\gamma$ -butyrolactone moiety to give **25** and the undesired diastereomer **24**. The authors proposed that the methoxy group controls the stereoselectivity of cyclization, in which the tertiary radical approached the butenolide moiety from the opposite face. A subsequent two-step sequence led to 8-oxoasperparaline C (**26**) from **25**.

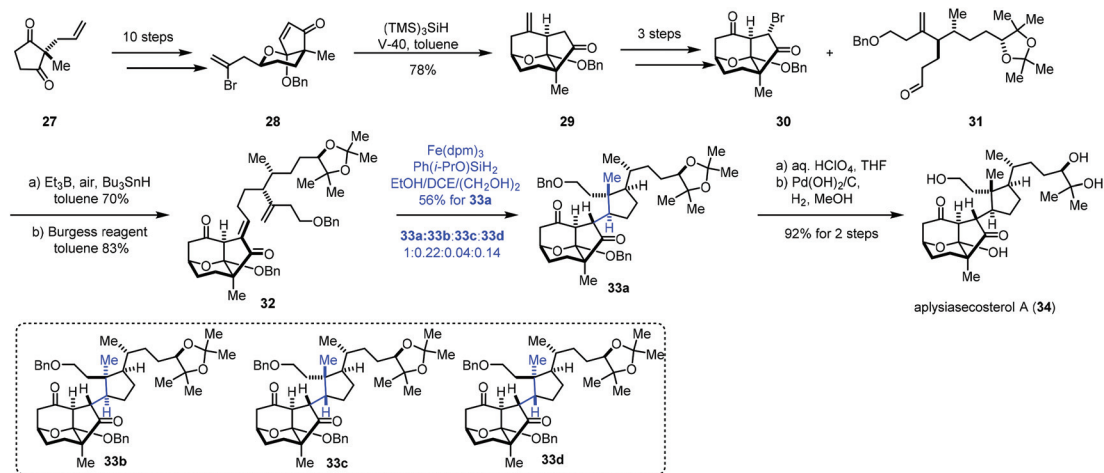
In 2018, Li and co-workers employed MHAT-based radical cyclization to complete the synthesis of aplysiasecosterol A (**34**) (Scheme 4).<sup>18</sup>  $\alpha,\beta$ -Unsaturated enone **28** could be obtained from **27** *via* a ten-step sequence. An intramolecular radical cyclization took place under the conditions of V-40 and (TMS)<sub>3</sub>SiH furnishing the tricyclic scaffold **29**. Subsequently, a three-step sequence provided **30**. Coupling of **30** and another



Scheme 3 Jahn's synthesis of 8-oxoasperparaline C (**26**).



Scheme 2 Maimone's synthesis of andrastin and terretinin meroterpenes.



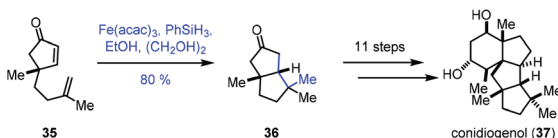
**Scheme 4** Li's synthesis of aplysiasesterol A (34).

segment 31 under the Oshima conditions let to an *anti*-aldol product, which was dehydrated to give 32. Initially, the authors tried the conditions (Fe(acac)<sub>3</sub>, PhSiH<sub>3</sub>, EtOH/(CH<sub>2</sub>OH)<sub>2</sub>) reported by Baran, and a mixture of four cyclization products (33a–33d) was obtained in 60% yield, in which the desired product 33a was obtained in just 25% yield due to the poor diastereoselectivity (33a:33b:33c:33d = 1:0.33:0.47:0.58). Switching the silicon reagent to the more reactive Ph(*i*-PrO)SiH<sub>2</sub> used by Shenvi improved the diastereoselectivity (33a:(33b + 33c + 33d) = ca. 1:1). The authors then screened other iron complexes. They observed that the more bulky 1,3-diketone ligands like diisobutylmethanate (dibm) and dipivaloylmethanate (dpm) gave better stereoselectivity (33a:(33b + 33c + 33d) = ca. 1.7–2.5:1). Finally, under the optimal conditions (Fe(dpm)<sub>3</sub>, Ph(*i*-PrO)SiH<sub>2</sub>, and EtOH/DCE/(CH<sub>2</sub>OH)<sub>2</sub>), 33a was prepared in 56% yield. Aplysiasesterol A (34) was

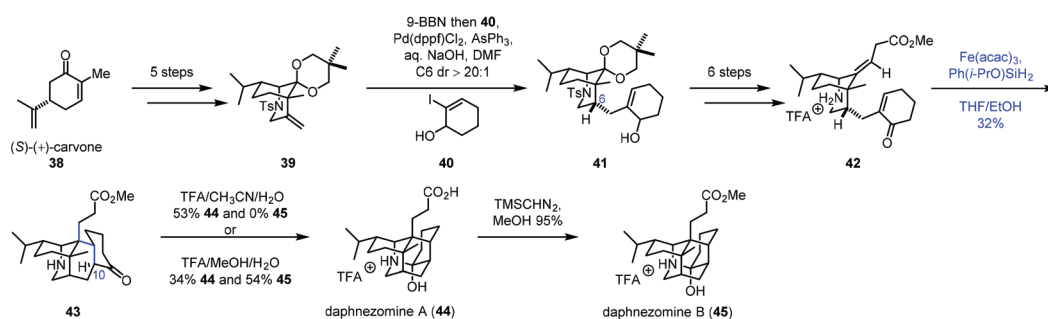
obtained from 33a in two steps including acetone hydrolysis and debenzoylation.

In 2019, Snyder reported the synthesis of conidiogenol (37) by a quaternary-centre-guided synthetic strategy (Scheme 5).<sup>19</sup> They employed radical conjugate addition initiated by iron-catalyzed HAT to furnish the bicyclic ketone 36 as a single diastereomer.

In 2020, Li and co-workers employed radical cyclization *via* iron-catalyzed HAT to accomplish the synthesis of (–)-daphnezomines A (44) and B (45) (Scheme 6).<sup>20</sup> In practice, carvone was transformed to 39 *via* a five-step sequence. Upon exposure of 39 to 9-BBN, followed by Suzuki–Miyaura coupling with 40, desired 41 was obtained. Treatment of 41 with a six-step sequence gave 42. To build the core skeleton structure, they tried *ene* cyclization and anionic cyclization, which turned out to be unfruitful. They finally resorted to MHAT-based radical cyclization. Under the conditions developed by Baran (Fe(acac)<sub>3</sub>, PhSiH<sub>3</sub>, and EtOH), the *trans*-fused adduct 43 was afforded in 16% yield as a single product. The authors proposed that the C10–H of 43 was delivered from the ammonium proton of 42 *via* a 1,5-proton transfer, which accounts for the *trans*-fused ring junction. Further screening of the conditions revealed that the desired cyclization product 43 could be prepared in 32% yield under the conditions of Fe(acac)<sub>3</sub> and



**Scheme 5** Snyder's synthesis of conidiogenol (37).



**Scheme 6** Li's synthesis of (–)-daphnezomines A (44) and B (45).

Ph(*i*-PrO)SiH<sub>2</sub> in THF/EtOH. The fact that the radical pathway worked in this case is perhaps a testament to its insensitivity to steric crowding.<sup>7b</sup> Lastly, in the presence of TFA, **43** was transformed to daphnezomines A (**44**) and B (**45**).

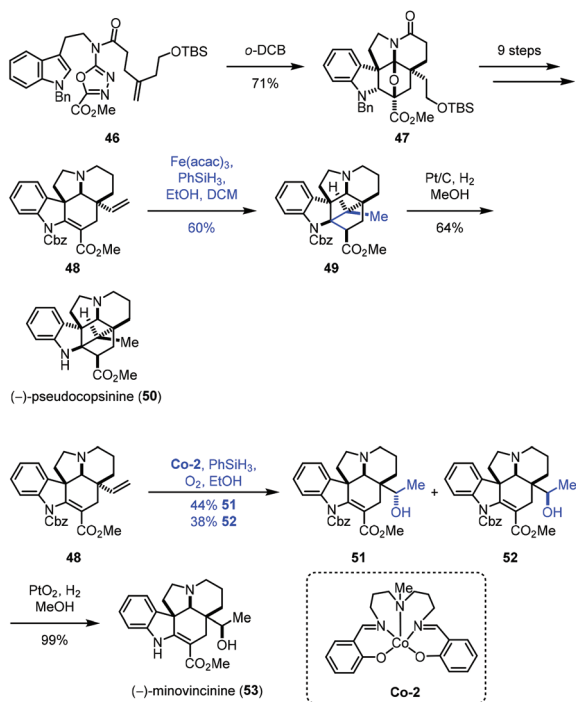
In 2020, Boger and co-workers disclosed the synthesis of (–)-pseudocopsinine (**50**) and (–)-minovincinine (**53**) (Scheme 7).<sup>21</sup> They employed the diene **48** as the common intermediate, from which different MHAT conditions were adopted to approach the target molecules. A sequential intramolecular [4 + 2] cycloaddition and [3 + 2] cycloaddition of **46** led to **47**, which was followed by functional group transformations to give the key intermediate **48**. Treatment of **48** with Fe(acac)<sub>3</sub> and phenylsilane provided **49** and its undesired epimer in 80% yield with good diastereoselectivity (3 : 1), favoring **49**. The authors observed that the yield of the cyclization increased with increasing Fe(acac)<sub>3</sub> catalyst (1.5 vs. 0.5 equiv.) and time (2 vs. 16 h) and using a less reactive silicon reductant (PhSiH<sub>3</sub> vs. Ph(*i*-PrO)SiH<sub>2</sub>). (–)-Pseudocopsinine (**50**) was then obtained from **49** under conditions of Pt/C and H<sub>2</sub>. Meanwhile, treating **48** with the Co catalyst **Co-2** furnished a pair of hydration products, the desired diastereomer **51** and its epimer in a nearly 1 : 1 ratio. Other attempted metal complexes such as Mn(acac)<sub>3</sub>, Fe<sub>2</sub>(ox)<sub>3</sub>, FePc, Fe(NO<sub>3</sub>)<sub>3</sub>, Fe<sub>2</sub>(SO<sub>4</sub>)<sub>3</sub>, Fe(acac)<sub>3</sub>, Fe(dpm)<sub>3</sub> and Co(acac)<sub>2</sub> all gave inferior results. (–)-Minovincinine (**53**) was formed after deprotection of **52**.

In 2021, Ma and co-workers achieved the synthesis of dankasterones A (**65**) and B (**66**) and periconiastone A (**67**) (Scheme 8).<sup>22</sup> They employed Co-catalyzed HAT-based radical cyclization to furnish a [6,6,6,5] tetracyclic core. Fragment **55**

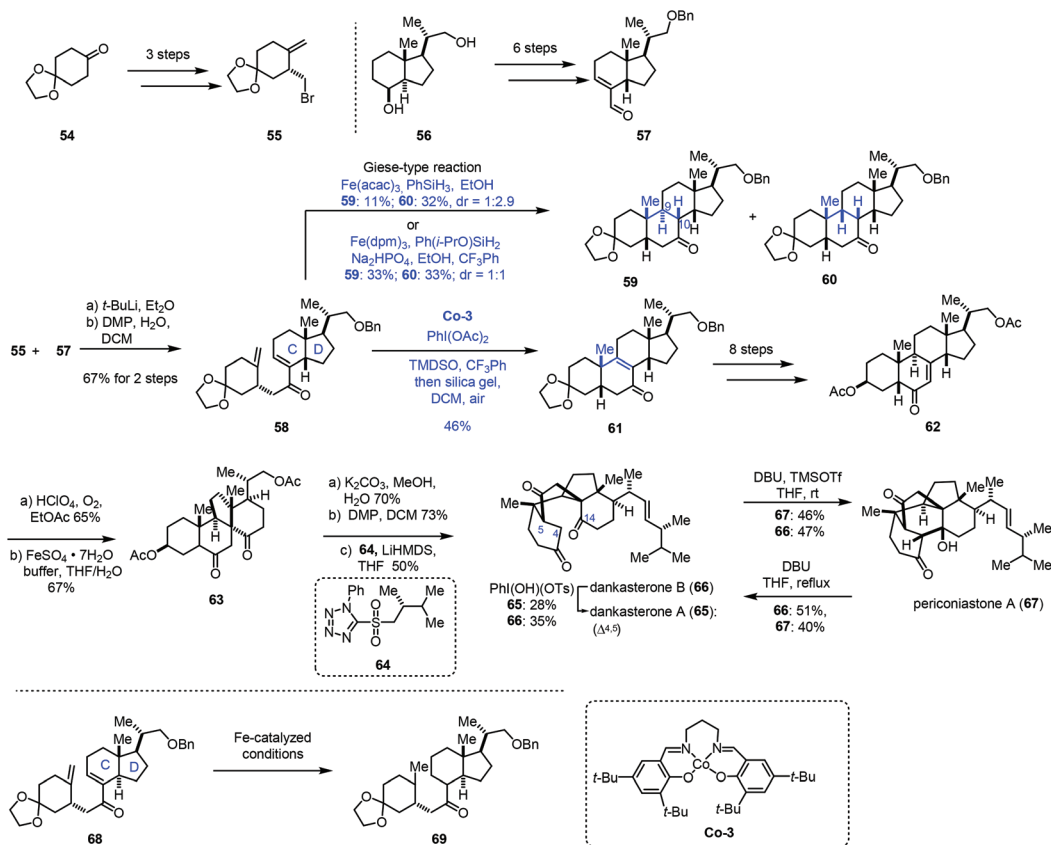
could be prepared from **54** *via* a three-step sequence. In parallel, fragment **57** was afforded from **56** in six steps. **55** and **57** were coupled through halogen lithium exchange and nucleophilic addition, which was followed by oxidation to give enone **58**. Exposure of the *cis*-fused C/D ring substrate **58** to Fe-catalyzed HAT conditions (Fe(acac)<sub>3</sub>, PhSiH<sub>3</sub>, EtOH) gave a pair of diastereomers **59** and **60** (dr = 1 : 2.9) *via* Giese-type radical conjugate addition, favoring undesired **60**. Screening of different Fe(III) catalysts, silane reagents, additives, solvents and temperatures showed that the optimal conditions (Fe(dpm)<sub>3</sub>, Ph(*i*-PrO)SiH<sub>2</sub>, Na<sub>2</sub>HPO<sub>4</sub>, EtOH, and CF<sub>3</sub>Ph) resulted in better diastereoselectivity (dr = 1 : 1). Since the yield of the desired cyclization product **59** from a Giese type reaction mediated by Fe was still low, the authors extended the catalyst to Mn and Co. While the Mn-catalyzed systems used were messy, subjecting **58** to Co-3-catalyzed HAT conditions with an *N*-fluoropyridinium oxidant afforded the cycloisomerization product **61** in 23–27% yield. Screening of oxidants revealed that PhI(OAc)<sub>2</sub> was optimal, delivering **61** in 46% yield. In this conversion, PhI(OAc)<sub>2</sub> might serve as the oxidant to oxidize Co(II) to Co(III) and facilitate the dehydrogenation. It is noteworthy that, in contrast to the *cis*-fused C/D ring substrate **58**, they found that the *trans*-fused C/D ring substrate **68** under Fe-catalyzed HAT conditions just gave the bis-reduced product **69** without cyclization. Enone **62** was then furnished from **61** in eight steps. Through C–H oxidation and radical rearrangement, **63** was afforded. Lastly, deacetylation, oxidation and Julia–Kocienski olefination gave dankasterone B (**66**), which could be transformed into dankasterone A (**65**) and periconiastone A (**67**).

In their synthetic studies towards wortmannin, Zhou and co-workers used HAT-based radical cyclization to install the tetracyclic core of wortmannin with an Fe catalyst (Scheme 9).<sup>23</sup> Their findings also demonstrated that a *cis*-fused C/D ring was the key to the desired cyclization since they observed that the substrate containing a *trans*-fused C/D ring failed to produce the desired product under the same conditions.

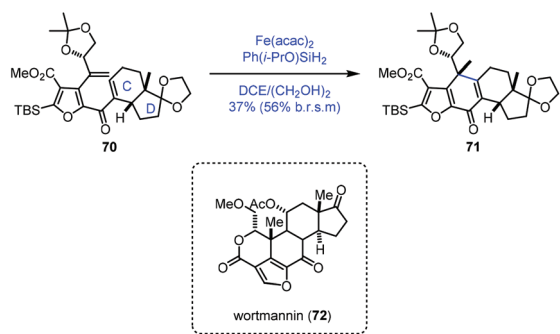
In 2017, Liu and co-workers accomplished the synthesis of hispidanin A (**82**),<sup>24,25</sup> in which they creatively employed iron-catalyzed radical polyene cyclization to furnish *trans*-decalin (Scheme 10). Compound **74** could be provided from **73** in four steps. Coupling **74** with Grignard reagent **75** in the presence of FeCl<sub>3</sub> afforded **76**. Oxidative operation of furan of **76** and a subsequent rearrangement provided the cyclization precursor **77**. Under the conditions of Co(acac)<sub>2</sub> or Mn(dpm)<sub>3</sub> as the catalyst, no desired product was detected probably because of the failure of radical initiation at the terminal alkene. Switching the catalyst to Fe(acac)<sub>3</sub> resulted in the desired radical polyene cyclization, giving the tricyclic compound **78** with 45% yield over 2 steps, along with an inseparable mixture of another three diastereomers in 19% combined yield. In this conversion, the radical initiated at the *gem*-disubstituted alkene went through a stereoselective cascade radical polycyclization process. As a result, the desired *trans*-decalin architecture bearing four contiguous stereogenic centers was obtained as



**Scheme 7** Boger's synthesis of (–)-pseudocopsinine (**50**) and (–)-minovincinine (**53**).



**Scheme 8** Ma's synthesis of dankasterones A (65) and B (66) and periconiastone A (67).



**Scheme 9** Zhou's synthesis of the tetracyclic core of wortmannin.

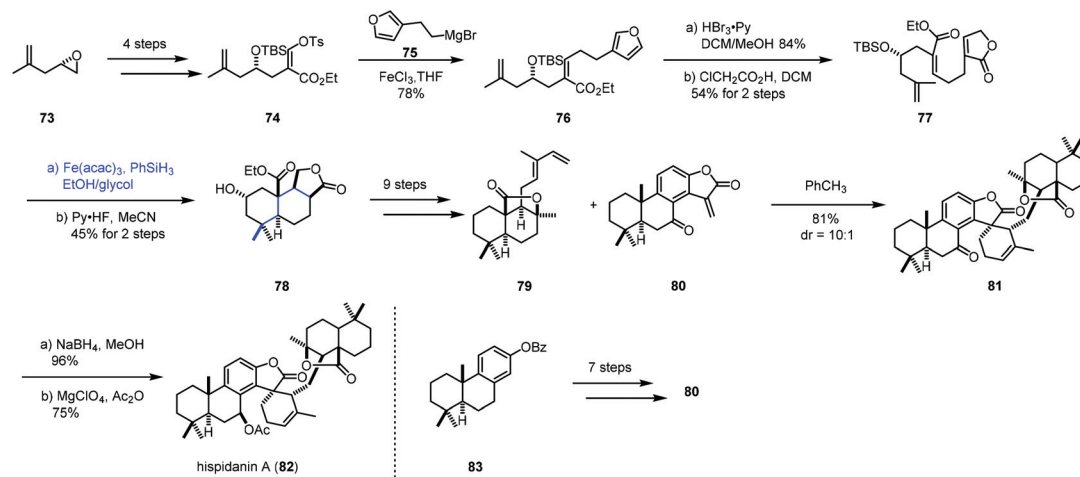
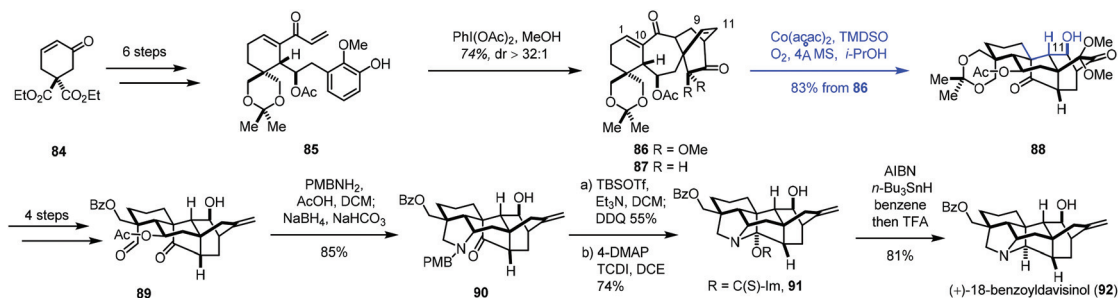
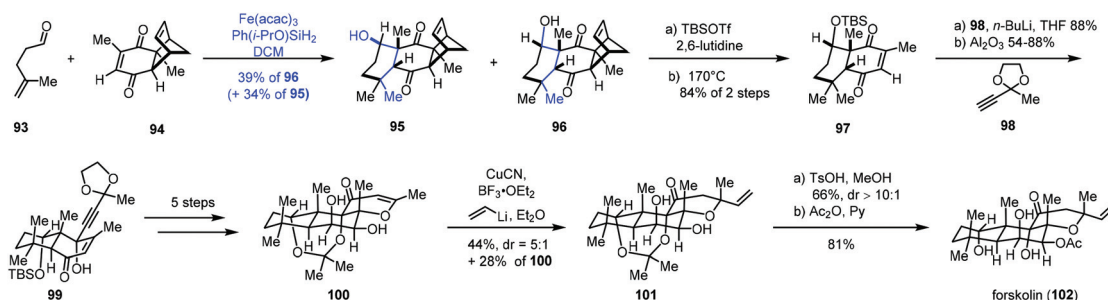
the major product. In comparison, Pattenden's work<sup>26</sup> showed that the *cis*-isomer was isolated as the major product when an acyl radical initiated the polyene process with a similar substrate. After nine steps of transformations from 78, 79 was obtained. At the same time, the dienophile fragment 80 was constructed using Yamamoto's cationic polyene cyclization. Next, a Diels–Alder cycloaddition between diene 79 and dienophile 80 occurred, furnishing 81. Reduction with NaBH<sub>4</sub> followed by acetylation gave hispidanin A (82).

Very recently, Ding and co-workers communicated the synthesis of (+)-18-benzoyldavisinol (92) featuring a HAT-initiated transannular redox radical cyclization (Scheme 11).<sup>27</sup>

Commercially available cyclohexenone 84 could be advanced to 85 in six steps. An oxidative dearomatization-induced-Diels–Alder cycloaddition furnished 86. Additional transformations gave 87. Initially, the authors expected to achieve reductive radical cyclization with an epoxide precursor (epoxidation of C9–C11 double bonds); however, the epoxidation of 87 was difficult. As such, the authors resorted to MHAT-based radical cyclization to create the core skeleton. After using the Fe catalysts, the expected cyclization products were not obtained.

They observed a hydration reaction occurring at the C1–C10 olefin of 86 under Mn(acac)<sub>2</sub> conditions, giving the corresponding alcohol at the C10 position. Encouraged by the results, the authors began to investigate Co catalysts. They found that the expected radical cyclization reaction took place from 86 under the conditions (Co(acac)<sub>2</sub>, TMSO, *i*-PrOH, O<sub>2</sub>, 4 Å MS), giving 88 in 83% yield. The reaction is remarkable as two highly strained rings and three contiguous stereogenic centers were created in the cascade process. With 88 in hand, a four-step sequence and a reductive amination reaction furnished 90. (+)-18-Benzoyldavisinol (92) was then prepared *via* hemiaminal formation and ensuing deoxygenation.

In 2019, Pronin and co-workers developed a new intermolecular annulation method between α,β- and γ,δ-unsaturated carbonyl compounds to furnish six-membered carbocycles through MHAT-initiated radical-polar crossover reaction. By taking advantage of the new method, they com-

Scheme 10 Liu's synthesis of hispidanin A (**82**).Scheme 11 Ding's synthesis of (+)-18-benzoyldavisinol (**92**).Scheme 12 Pronin's synthesis of forskolin (**102**).

pleted the synthesis of forskolin (**102**) (Scheme 12).<sup>28</sup> A radical tandem reaction between  $\gamma,\delta$ -unsaturated aldehyde **93** and enone **94** gave cyclization products **95** and desired **96** as a pair of diastereomers (dr = 1:1). Although the diastereoselectivity was low, the reaction was scalable and allowed for the production of multigram quantities of **96**. In addition, the undesired epimer **95** could be converted to **96** after an oxidation and reduction process in 87% yield. Treatment of **96** with a two-step sequence including protection and retro-Diels–Alder reaction, followed by nucleophilic addition and epimerization, gave **99**. After five steps, **99** could be transformed to **100**.

Forskolin (**102**) was then afforded through conjugate addition, deprotection and acetylation.

## 2.2 Hydroarylation

In addition to electron-deficient olefins corresponding to conjugate addition, aryl groups could be used as the terminator in MHAT reactions. We will systematically introduce applications of hydroarylations of unactivated olefins triggered through MHAT-based reactions in this section. Traditional methods such as Friedel–Crafts alkylation usually require vigorous reaction conditions to activate olefins.<sup>29</sup> There are also many

reports showing transition metal-mediated addition of aromatic C–H bonds across olefins with high regio- and chemoselectivity.<sup>30</sup> While metal catalysts usually involve expensive and toxic metals, compared to the above methods, MHAT-based hydroarylations would serve as an alternative to hydroarylation of unactivated olefins.

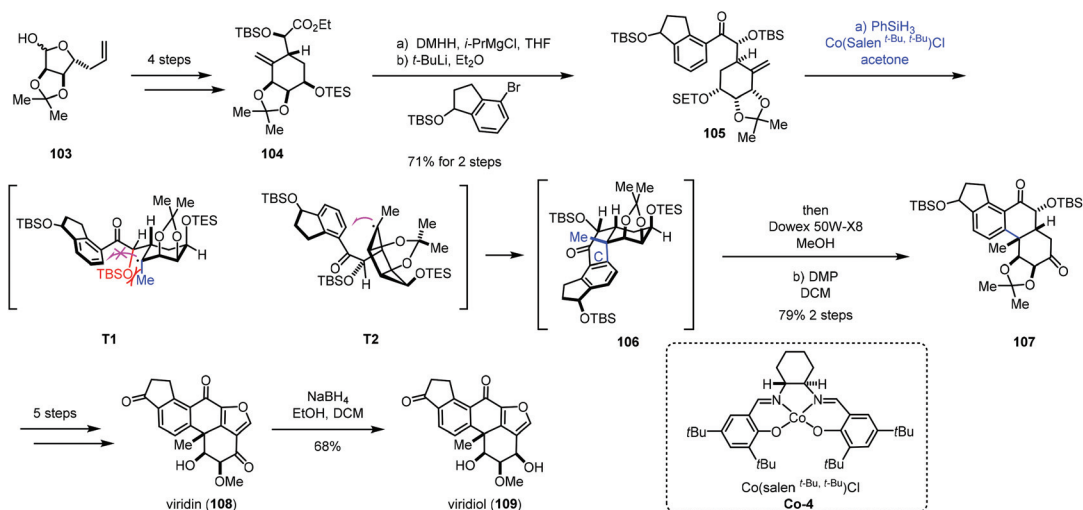
In 2019, Gao and co-workers completed the total synthesis of viridin and viridiol,<sup>31</sup> in which they employed Co-catalyzed hydroarylation reaction to close the C-ring (Scheme 13). Their synthesis commenced with **104**, which was prepared from **103** via a four-step sequence. Treatment of **104** with DMHH and *i*-PrMgBr afforded Weinreb amide, which was attacked by aryl lithium to furnish **105**. Under conditions of **Co-4** and PhSiH<sub>3</sub>, the intramolecular radical hydroarylation occurred to form the tetracyclic core **106** with excellent diastereoselectivity. The authors rationalized the stereochemistry of MHAT cyclization through analysis of the radical intermediates **T1** and **T2**. There is a steric effect between the OTBS and the methyl in **T1** and no such effect in **T2**. Therefore, the intermediate **T2** is a favorable transition state to generate the tetracyclic core **106**. Sequential deprotection and oxidation delivered **107**. Five additional steps were carried out to give viridin (**108**). Viridin (**108**) could be converted to viridiol (**109**) by selective reduction.

Recently, Gao and co-workers accomplished the synthesis of norzoanthamine using the same hydroarylation strategy to create the tetracyclic core (Scheme 14).<sup>32</sup> A carvone derivative could be converted into **111** in nine steps. Ueno–Stork radical cyclization furnished **112** through radical conjugate addition. **112** went through a three-step sequence to deliver aldehyde **113**, which was reacted with Grignard reagent **114**, followed by acetylation to afford compound **115**. Treatment of **115** with Co-catalyzed hydroarylation conditions reported by Shenvi gave the tetracyclic core **116** after deprotection of TBS. Subsequent Birch reduction and acetylation led to **117**. The following task was hydrogenation of the *tetra*-substituted olefin. The authors

proposed that the desired product with the *trans-anti-trans*-fused perhydrophenanthrene A–B–C ring was more thermodynamically stable than other relative configurations, so the *anti*-addition of hydrogen was expected. Subjecting **117** to Shenvi's hydrogenation conditions (Mn(dpm)<sub>3</sub> and PhSiH<sub>3</sub>) afforded **118** with a *trans*-fused A–B ring with good diastereoselectivity but low yield.

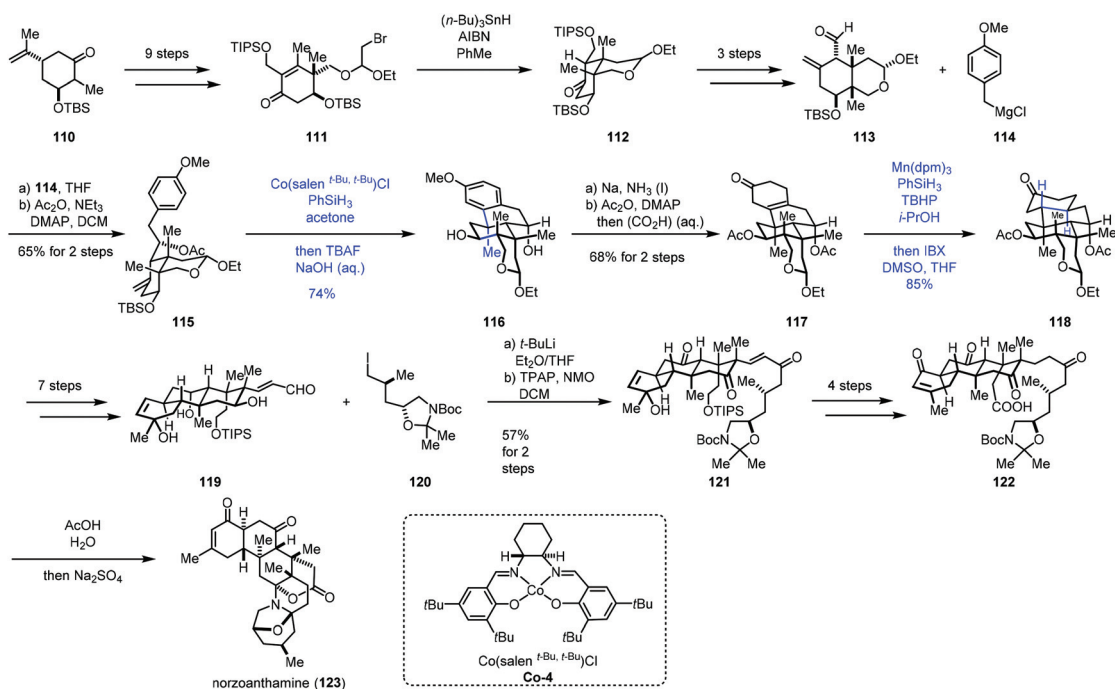
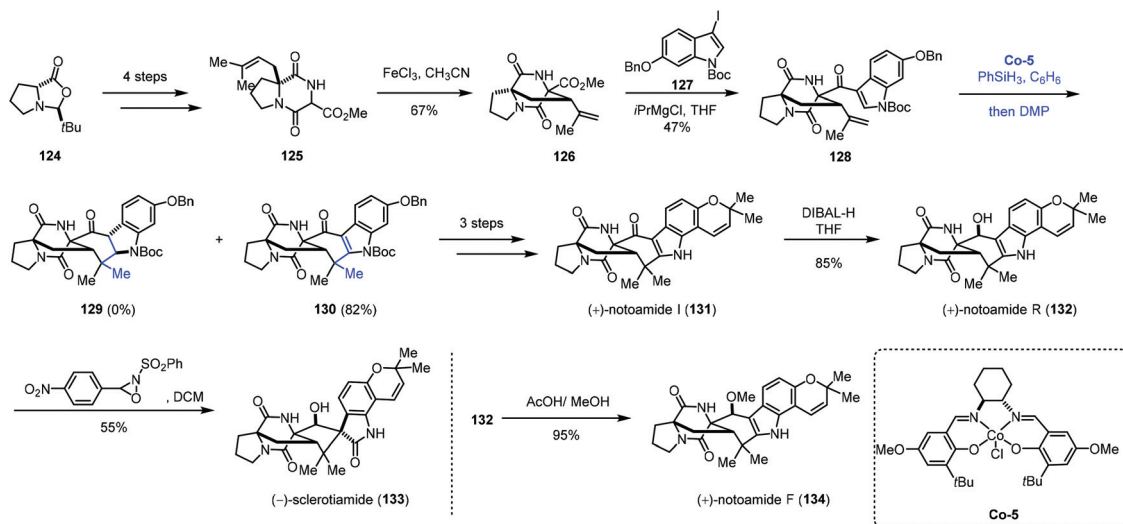
After optimization, the authors discovered that excess of PhSiH<sub>3</sub> (>4.0 equiv.) and *t*-butyl hydroperoxide (>4.0 equiv.) could ensure the complete conversion of **117**, accompanied by the reduction of the carbonyl group. Subsequent oxidation gave **118** with 85% yield. **118** could be transformed to the unsaturated aldehyde **119** in seven steps. Reaction of **120** and aldehyde **119** followed by oxidation gave rise to ketone **121**. **122** was then prepared from **121** in four steps. Deprotection of **122** followed by bis-aminoacetalization gave norzoanthamine (**123**).

Besides phenyl groups, indoles have also been used as radical acceptors in MHAT-based reactions. In 2016, Li and co-workers employed cobalt-catalyzed HAT reaction to achieve desired cyclization in the total syntheses of (+)-notoamides **F** (**134**), **I** (**131**), and **R** (**132**) and (–)-sclerotiamide (**133**) (Scheme 15).<sup>33</sup> The starting material **124** was subjected to the reaction to give **125** in four steps. Under the optimal conditions, bicyclo[2,2,2]diazaoctane **126** was formed through oxidative aza-Prins cyclization with FeCl<sub>3</sub>. The reaction of **126** with **127** delivered ketone **128**. With Shenvi's method, the desired product could not be obtained. While switching the cobalt catalyst to **Co-5**, the authors were able to obtain the desired products **130** along with 2,3-dihydroindole **129**, both in poor yields. After optimization, they discovered that using a slight excess of PhSiH<sub>3</sub> would increase the yields of **129** and **130**, and they also envisioned that **129** could be elaborated to **130** through oxidation. Thus, when using the optimized conditions and quenching the reaction mixture with Dess–Martin periodinane (DMP), **130** was synthesized in 82% yield. In this



Scheme 13 Gao's synthesis of viridin (**108**) and viridiol (**109**).

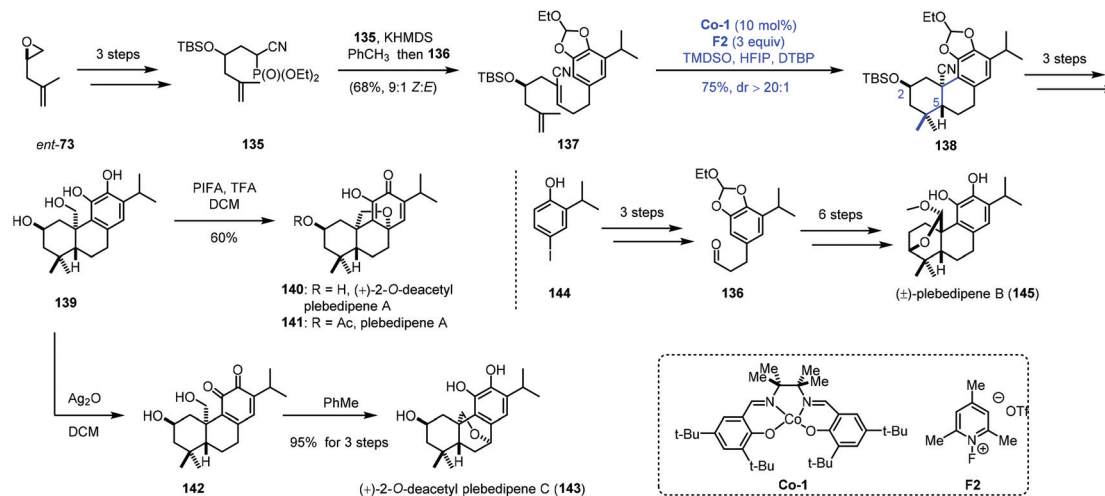


Scheme 14 Gao's synthesis of norzoanthamine (**123**).Scheme 15 Li's synthesis of (+)-notoamides F (**134**), I (**131**), and R (**132**) and (-)-sclerotiamide (**133**).

reaction, the indole moiety is the radical acceptor. Compound **130** could be converted to (+)-notoamides F (**134**), I (**131**), and R (**132**) and (-)-sclerotiamide (**133**) featuring an allenyl Claisen rearrangement.

MHAT-initiated polyene cyclization was extensively investigated by Vanderwal and co-workers. They employed this strategy to complete the synthesis of a few oxidized abietane diterpenoids (Scheme 16).<sup>34</sup> In their synthesis, *ent*-73 as the starting material was transformed to **135** via epoxide ring opening and hydroxyl protection. Another fragment **136** was furnished from

**144**. Next, **135** was reacted with **136** to deliver the bicyclization precursor **137**. With Co-1 as the catalyst, TMDSO as the hydrogen source and 2,6-di-*tert*-butylpyridine (DTBP) as the additive, a bicyclization took place via a radical process giving **138**. The reaction process was similar to that in Liu's work,<sup>24,25</sup> and the chiral center C2 would control the stereochemistry of the radical bicyclization. In particular, in their studies with model substrates, the authors found that oxygen substitution at C2 was associated with efficient polyene cyclization (>81% yield, *dr* > 20 : 1) for the equatorial group with both the free hydroxyl



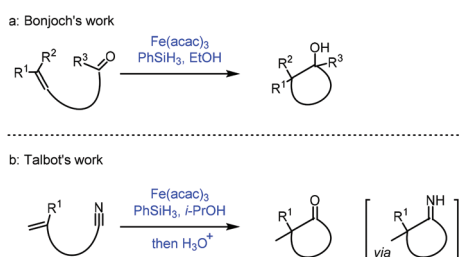
**Scheme 16** Vanderwal's synthesis of (+)-2-O-deacetyl plebedipenes A (**140**) and C (**143**), and plebedipene B (**145**).

group and its corresponding silyl ether. The common intermediate **139** was then afforded through continuous reduction and deprotection. (+)-2-O-Deacetyl plebedipene A (**140**) was eventually obtained by oxidation of **139** with PIFA, and (+)-2-O-deacetyl plebedipene C (**143**) was obtained by oxidation with Ag<sub>2</sub>O. Plebedipene B (**145**) could be obtained from **136** through similar reactions.

### 2.3 Reductive coupling with carbonyl or cyano functionalities

The reductive coupling of an olefin to a carbonyl functionality has been reported.<sup>35a</sup> Most of these reductive coupling reactions have been carried out under a hydrogen atmosphere in the presence of precious metal catalysts such as Rh. In 1989, Mukaiyama reported Co-catalyzed reductive coupling of  $\alpha,\beta$ -unsaturated nitrile with aldehydes in the presence of phenylsilane.<sup>35b</sup>

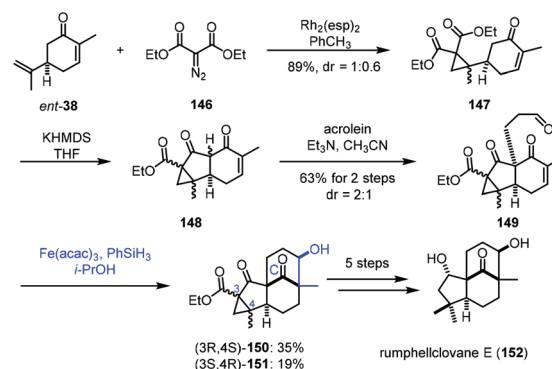
In 2018, Bonjoch<sup>36a</sup> and Talbot<sup>36b</sup> independently disclosed their accomplishment in MHAT reactions. They extended the radical acceptor to ketone and cyano groups when unactivated olefins were employed. Bonjoch discovered that the radical-centered carbon center from MHAT to the olefin was able to attack the proximal ketone group giving the corresponding tertiary alcohol (Scheme 17a), while Talbot observed that the resulting carbon radical would attack the cyano group leading to a ketone *via* an imine intermediate (Scheme 17b).



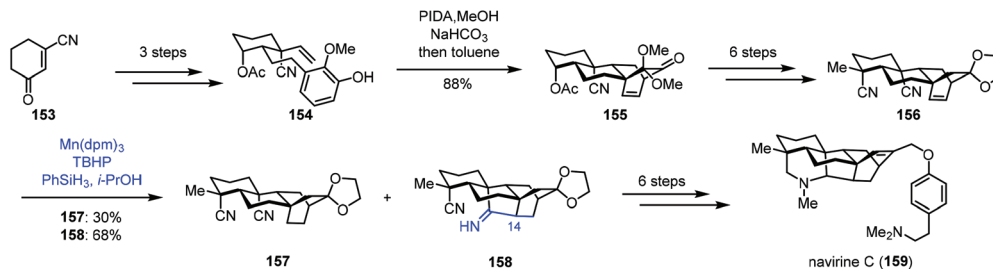
**Scheme 17** (a) Bonjoch's work and (b) Talbot's work.

In 2021, Liu and co-workers applied iron-catalyzed reductive aldol reaction in the synthesis of rumphecllovane E (**152**) (Scheme 18).<sup>37</sup> Cyclopropanation between *ent*-**38** and **146** catalyzed by Rh<sub>2</sub>(esp)<sub>2</sub> afforded **147**, which could be transformed to **149** *via* acylation and Michael addition. To assemble the tetracyclic core, they tried different reductive aldol conditions including Rh, Pd or Cu as catalysts, and all attempts failed. The authors thus resorted to MHAT-based conditions. The conditions of Mn and Co catalysts did not afford the desired cyclization product. Fortunately, a tetracyclic compound was obtained by the Fe-catalyzed radical process. After optimization, the authors observed that the treatment of **149** with Fe(acac)<sub>3</sub> and PhSiH<sub>3</sub> in *i*-PrOH led to the desired products **150/151**. With respect to the mechanism, the authors proposed that MHAT to enone **149** provides the radical intermediate, which is further reduced by Fe(II) to provide the enolate, which reacts with the aldehyde through an aldol process to form tetracyclic **150/151**. Next, a five-step transformation furnished rumphecllovane E (**152**).

In 2018, Ma and co-workers reported the synthesis of navirine C (**159**) (Scheme 19).<sup>38</sup> Their synthesis started with **153**,



**Scheme 18** Liu's synthesis of rumphecllovane E (**152**).



Scheme 19 Ma's synthesis of navirine C (159).

which could be transformed to **154** via a three-step sequence. Oxidative dearomatization of **154** and Diels–Alder cycloaddition gave **155**. Then dinitrile **156** was obtained in six steps. Under MHAT reaction conditions ( $\text{Mn}(\text{dpm})_3$ ,  $\text{PhSiH}_3$ , and TBHP) reported by Shenvi and co-workers, the desired reductive cyclization occurred, delivering **158** in 68% yield, along with the reduction product **157** in 30% yield. The authors proposed that  $\text{HMn}(\text{dpm})_2$  reacted with an alkene to produce the corresponding C14 radical intermediate, which might attack the cyano group to produce the cyclized intermediate. Further reduction generated **158**. An additional six-step sequence gave avirine C (**159**).

Talbot's method was subsequently used by Zhai and co-workers in their synthesis of (–)-conidiogenone B (**166**), (–)-conidiogenone (**167**), and (–)-conidiogenol (**168**) (Scheme 20).<sup>39</sup> The starting material **160** could be transformed to **161** via a three-step sequence involving Corey–Bakshi–Shibata reduction, tandem vinyl etherification/Claisen rearrangement, and van Leusen reaction. Under Talbot's conditions, alkene–nitrile cyclization was achieved, providing the bicyclic ketone **163**, which was elaborated to deliver **164** by an additional nine steps. Subsequently, ozonolysis, followed by aldol reaction, provided (–)-conidiogenone B (**166**). After epoxidation and reduction, (–)-conidiogenone (**167**) was prepared. Reduction of (–)-conidiogenone (**167**) gave rise to (–)-conidiogenol (**168**).

### 3. C–O bond formation

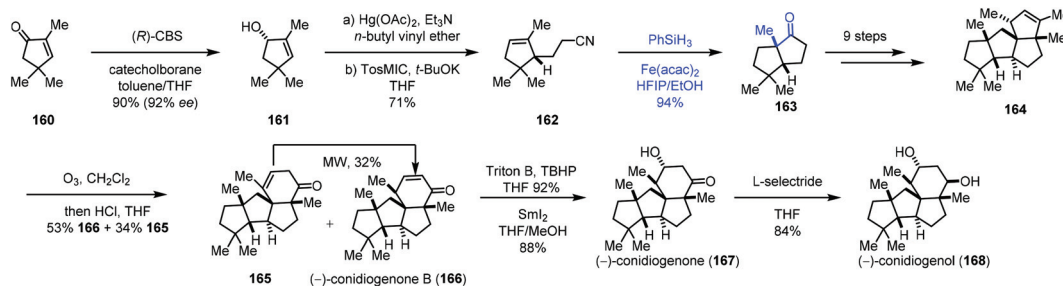
Mukaiyama developed the Co-catalyzed hydration of olefins in the presence of silane and oxygen in 1989.<sup>3</sup> Since then, the

reaction has seen applications in natural product synthesis.<sup>40,41</sup> In Shenvi's excellent review published in 2016, they carefully summarized examples of olefin hydration under MHAT conditions in natural product synthesis. So next we will mainly focus on the examples that appeared after 2016. Hydration and hydroperoxidation will be discussed separately.

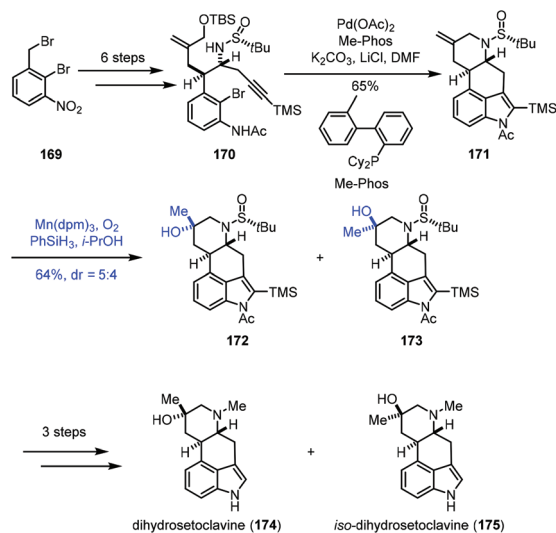
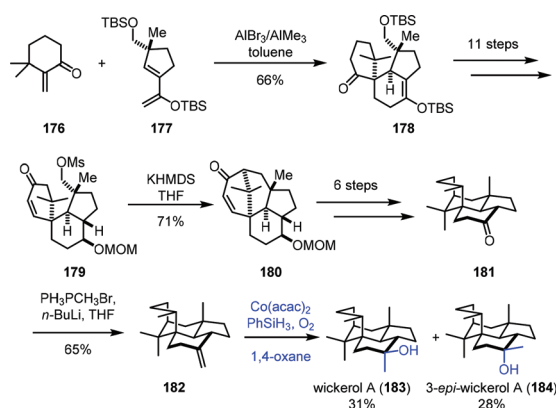
#### 3.1 Hydration

Mukaiyama hydration reaction is a mild way to hydrate exocyclic double bonds to obtain tertiary hydroxyl groups. In 2017, Jia and co-workers applied Mukaiyama hydration in their synthesis of dihydrosetoclavine (Scheme 21).<sup>42</sup> The starting material **169** was converted into **170** in six steps. Larock indole annulation of **170** afforded **171**. Under Mn-catalyzed Mukaiyama hydration conditions, a diastereomeric mixture of tertiary hydroxyl **172** and **173** was furnished. The authors noticed that using a similar substrate (changing the *tert*-butanesulfinyl group of **171** to  $\text{CO}_2\text{Me}$ ) with hydration conditions failed to give the desired hydration product, indicating that the carbamate moiety has a negative effect on the hydration. Dihydrosetoclavine (**174**) and *iso*-dihydrosetoclavine (**175**) were then synthesized in three steps.

In 2017, Trauner and co-workers employed Mukaiyama hydration at the last step to furnish wickerol A (**183**) (Scheme 22).<sup>43</sup> A Diels–Alder cycloaddition between the known enone **176** and diene **177** was performed to afford **178**. The key intermediate **179** could be accessed from **178** in necessary functional group transformations. Treatment of **179** with KHMDS induced intramolecular alkylation to provide **180**. Ketone **181** was afforded after the introduction of the missing methyl group. Initially, they carried out the methyl nucleophilic addition to the ketone carbonyl with methyl Grignard or



Scheme 20 Zhai's synthesis of (–)-conidiogenone B (**166**), (–)-conidiogenone (**167**), and (–)-conidiogenol (**168**).

Scheme 21 Jia's synthesis of dihydrosetoclavine (**174**).Scheme 22 Trauner's synthesis of wickerol A (**183**).

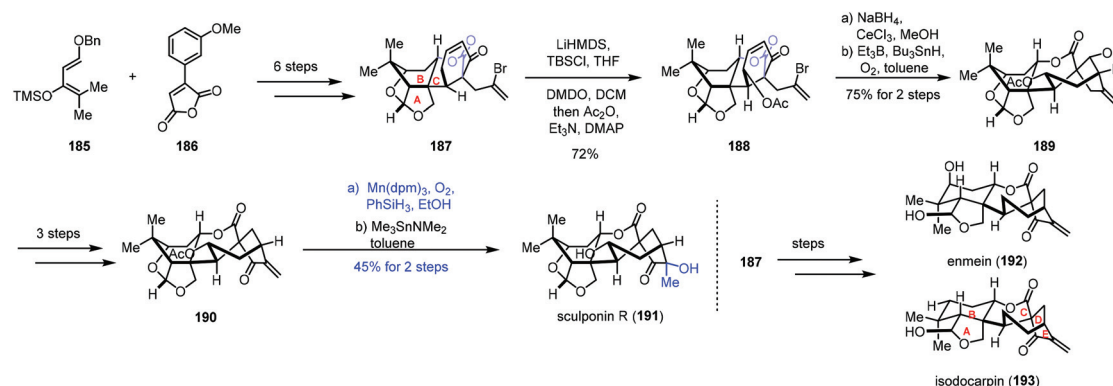
methylithium, but unfortunately, undesired 3-*epi*-wickerol A (**184**) was produced as the sole product. Addition of the Lewis acid MAD to the system still favored undesired **184** (**183** : **184** =

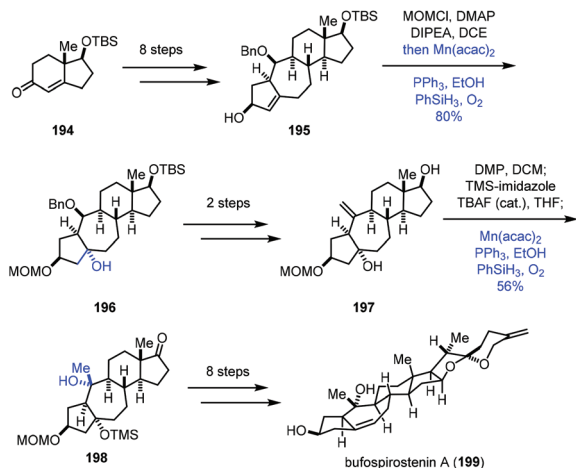
1 : 4). The authors ultimately found that a two-step transformation including Wittig reaction and Mukaiyama hydration gave a better ratio. Olefination of ketone led to **182**, which underwent Mukaiyama hydration reaction with  $\text{Co}(\text{acac})_2$  as the catalyst to afford wickerol A (**183**) and 3-*epi*-wickerol A (**184**) in an almost 1 : 1 ratio.

In 2018, a divergent total synthesis of enmein-type natural products was reported by Dong and co-workers (Scheme 23).<sup>44</sup> The common intermediate **187** containing the A/B/C rings of (–)-enmein (**192**), (–)-isodocarpin (**193**), and (–)-sculponin R (**191**) was synthesized from diene **185** and anhydride **186** involving Diels–Alder cycloaddition and Birch reduction.  $\gamma$ -Hydroxylation was achieved with vinylogous enol ether formation and DMDO oxidation to afford ester **188**, which was reduced by Luche reduction, followed by radical annulation to give **189**. A three-step conversion furnished **190**. Finally, functionalization of the exocyclic double bond was carried out under the Mn-catalyzed Mukaiyama hydration conditions ( $\text{Mn}(\text{dpm})_3$ ,  $\text{PhSiH}_3$ ,  $\text{O}_2$ , and  $\text{EtOH}$ ) to furnish (–)-sculponin R (**191**) after deacetylation in 45% yield over two steps. The common intermediate **187** could be also converted to (–)-enmein (**192**) and (–)-isodocarpin (**193**) in a few steps.

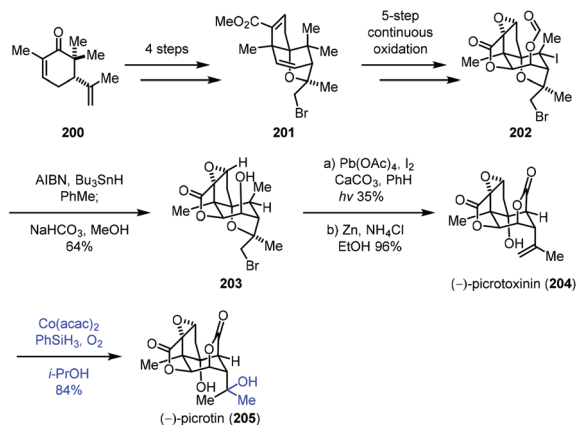
In 2020, Li and co-workers reported the synthesis of bufospirostenin A (**199**), in which Mukaiyama hydration was adopted two times (Scheme 24).<sup>45</sup> This synthesis began with **194**, which was transformed to tetracyclic **195** in eight steps. Treatment of **195** with  $\text{MOMCl}$ , followed by a standard Mukaiyama hydration ( $\text{Mn}(\text{acac})_2$ ,  $\text{PhSiH}_3$ ,  $\text{PPh}_3$ ,  $\text{O}_2$ , and  $\text{EtOH}$ ), gave the tertiary alcohol **196** in 80% yield. Afterwards, a two-step conversion furnished **197**, poised for another Mukaiyama hydration. Then the tertiary alcohol **198** with the desired configuration was furnished *via* the same hydration process from the exocyclic double bond of **197** in 56% yield. A further eight steps of transformation afforded the natural product bufospirostenin A (**199**).

In 2020, Shen reported the synthesis of picrotoxinin (**204**), which could be transformed to picrotin (**205**) by Mukaiyama hydration (Scheme 25).<sup>46</sup> Their synthesis commenced with **200**, which could be converted to **201** *via* a four-step sequence. **201** went through a five-step continuous oxidation process to

Scheme 23 Dong's synthesis of (–)-enmein (**192**), (–)-isodocarpin (**193**), and (–)-sculponin R (**191**).



Scheme 24 Li's synthesis of bufospirostenin A (199).



Scheme 25 Shenvi's synthesis of picrotoxinin (204) and picrotin (205).

give **202**. Treatment of **202** with AIBN and Bu<sub>3</sub>SnH removed the tertiary iodide, followed by the cleavage of the formyl group to furnish **203**. Picrotoxinin (**204**) was obtained from **203** through functionalization of the methyl group and cleavage of bromoether. Finally, a Mukaiyama hydration under Co(acac)<sub>2</sub>, PhSiH<sub>3</sub>, O<sub>2</sub>, and *i*-PrOH conditions installed the ter-

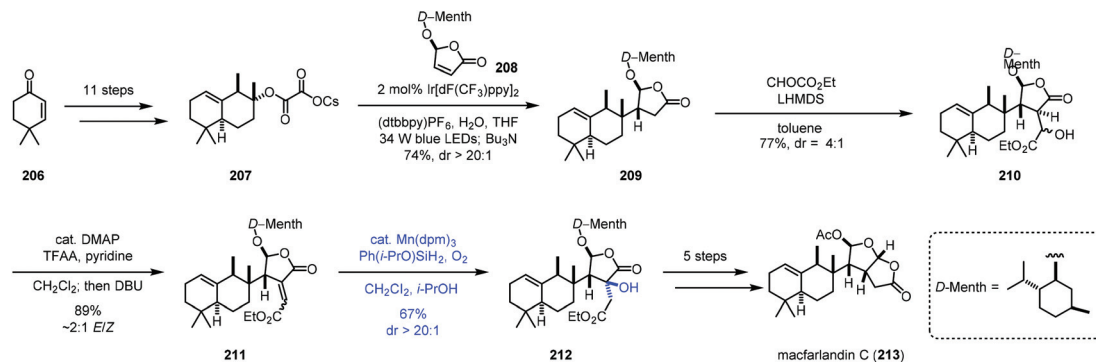
tiary hydroxyl from the exocyclic double bond of **204** to deliver the desired picrotin (**205**) in 84% yield.

In 2020, Overman and co-workers reported the synthesis of macfarlandin C (**213**), in which Mukaiyama hydration was used (Scheme 26).<sup>47</sup> The oxalate radical precursor **207** was obtained from **206** after eleven steps of transformations. Irradiation of **207** and *D*-menthol-derived chlorobutenolide **208** in the presence of an Ir-catalyst installed the vicinal quaternary and tertiary stereocenters generating **209**. Two more steps gave **211**. Mukaiyama hydration with Mn(dpm)<sub>3</sub> and Shenvi's more reactive Ph(*i*-PrO)SiH<sub>2</sub> and O<sub>2</sub> provided **212** in a regio- and stereoselective manner in 67% yield. In this case, the electron-rich olefin remained untouched. Macfarlandin C (**213**) was then obtained in five additional steps.

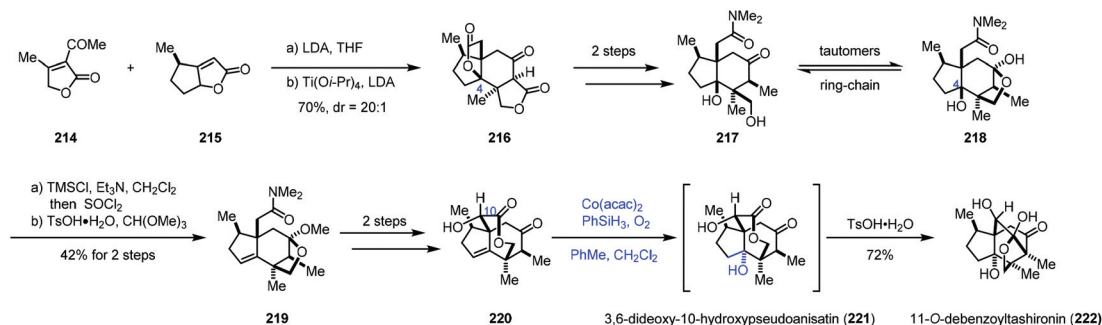
The above-mentioned examples are related to the hydration of exocyclic double bonds. Next, the hydration of endocyclic double bonds will be summarized.

In 2017, Shenvi and co-workers reported a seven-step synthesis of (–)-11-*O*-debenzoyltashironin (**222**) from butenolide (Scheme 27).<sup>49</sup> Butenolide heterodimerization of **215** to **214**, followed by the addition of titanium tetraisopropoxide and lithium diisopropylamide, gave tetracyclic **216**. To invert C<sub>4</sub>, the authors planned to eliminate the lactone to an alkene, and then use Mukaiyama hydration reaction to construct the tertiary hydroxyl group with the desired configuration. In accordance with the strategy, a two-step sequence afforded **217/218**, which was converted to **219** featuring a dehydration step. Seven-membered lactone **220** was afforded in two more steps. Mukaiyama hydration of the endocyclic double bond of **220** with Co(acac)<sub>2</sub> followed by the addition of *p*-toluenesulfonic acid produced **222** with a *trans*-hydrindane framework in 72% yield. *trans*-Hydrindane is thought to be thermodynamically disfavoured. The authors suspected that, in the current case, C<sub>10</sub> alcohol might determine the stereochemistry of hydration as C<sub>10</sub> alcohol shields the β-face. In addition, the authors mentioned that the hydration had to be arranged at the late stage since attempts with earlier intermediates resulted in a complex mixture or the undesired *cis*-hydrindane product.

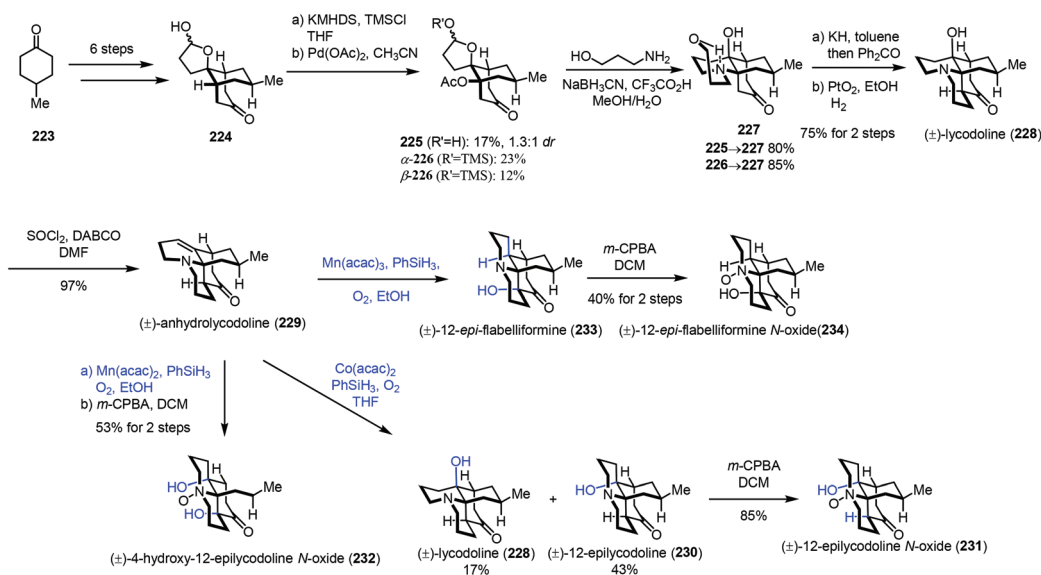
In 2017, Fan and co-workers communicated their synthesis of lycodoline-type *Lycopodium* alkaloids (Scheme 28).<sup>50</sup> In this case, subjecting the common intermediate anhydrolycodoline



Scheme 26 Overman's synthesis of macfarlandin C (213).



Scheme 27 Shenvi's synthesis of (-)-11-O-debenzoyltashironin (222).

Scheme 28 Fan's synthesis of lycodoline-type *Lycopodium* alkaloids.

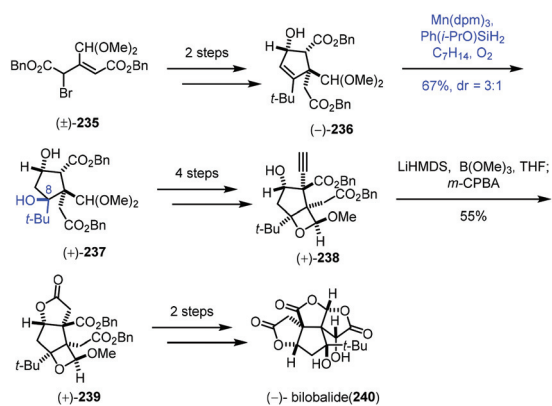
(229) to different hydration conditions could give different types of products. This synthesis commenced with the preparation of 224 from 4-methylcyclohexone 223. Treatment of 224 with  $\text{KHMDS}$  and  $\text{TMSCl}$ , followed by tandem oxidative dehydrogenation and oxa-Michael reaction, gave 225/226. Then tandem reductive amination and bridgehead aminolysis reaction were performed to give 227. Lastly, lycodoline (228) was obtained through a sequence of Oppenauer oxidation, aldol condensation and hydrogenation of the olefin. Anhydrolycodoline (229) was furnished *via* dehydration from lycodoline (228).

Under Mukaiyama hydration conditions with  $\text{Co}(\text{acac})_2$  in THF, anhydrolycodoline (229) could be elaborated to 12-epilycodoline (230) and lycodoline (228). 230 could be further oxidized with  $m$ -CPBA to provide 12-epilycodoline *N*-oxide (231). In comparison, when anhydrolycodoline (229) was treated with  $\text{Mn}(\text{acac})_2$  and phenylsilane in  $\text{EtOH}$ , followed by oxidation with  $m$ -CPBA, it turned out that not only the C=C double bond was hydrated, but also  $\alpha$ -hydroxylation occurred, providing 4-hydroxy-12-epilycodoline *N*-oxide (232). It is interesting to note that hydration with  $\text{Mn}(\text{acac})_3$  gave the  $\alpha$ -hydroxylation

product 12-*epi*-flabelliformine (233), which could be oxidized into 234.

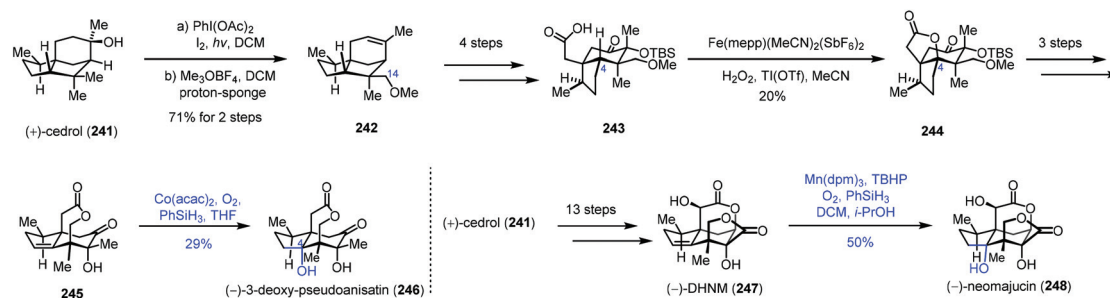
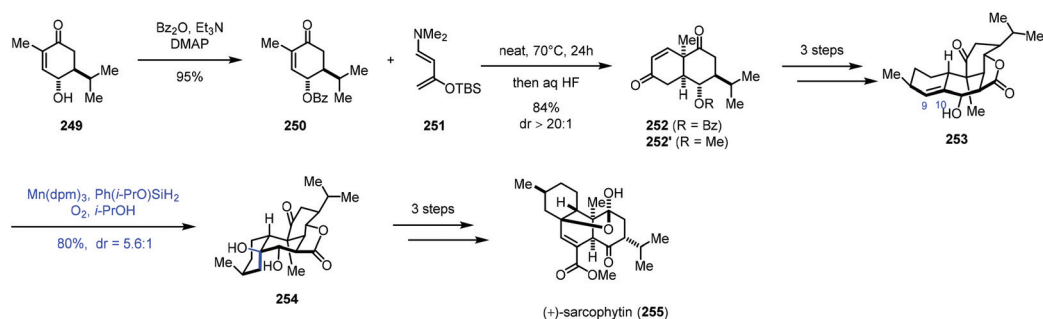
In 2019, Shenvi and co-workers described a solvent-controlled Mukaiyama hydration in total synthesis of (-)-bilobalide (240) (Scheme 29).<sup>51a,b</sup> In the process of the synthesis of bilobalide, with respect to the hydration step of 236 to 237, Shenvi and co-workers observed that there is strong correlation between solvent polarity and diastereoselectivity. For example, under standard Mukaiyama conditions,  $\text{Mn}(\text{dpm})_3/\text{PhSiH}_3/i\text{-PrOH}$ , 237 was delivered with no diastereoselectivity. Switching to  $\text{Ph}(i\text{-PrO})\text{SiH}_2$  and ethereal solvent such as *tert*-butyl methyl ether led to undesired diastereomer as the major product (dr = 1 : 1.8), while methylcyclohexane as solvent favoured the desired product 237 in a 3 : 1 ratio. An additional 4 steps gave 238. Shenvi and co-workers then developed a new method for alkyne oxidation to form 239. Finally, (-)-bilobalide (240) was accessed through a skeletal rearrangement and oxidation.

In 2019, Maimone and co-workers published a semisynthetic strategy to the *Illicium* sesquiterpenes from cedrol by their site-selective  $\text{C}(\text{sp}^3)\text{-H}$  bond functionalization reactions.



Scheme 29 Shenvi's synthesis of (-)-bilobalide (240).

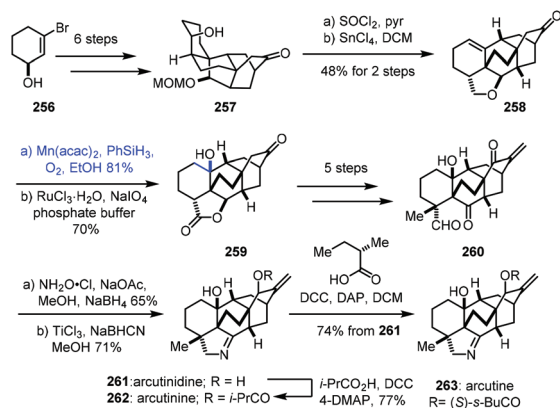
They employed Mn or Co-catalyzed hydration to install the C4 hydroxyl group (Scheme 30).<sup>52</sup> A hypiodite photolysis of **241** with  $\text{PhI(OAc)}_2$  and  $\text{I}_2$  furnished a strained tetrahydrofuran intermediate by oxidation of C14 of cedrol, which underwent alkylation and concomitant elimination to provide **242**. The C4 oxidation precursor **243** was furnished from **242** in four steps. Fe-Catalyzed selective C–H oxidation of C4 afforded **244**, which was then transformed to alkene **245**. Under Co-catalyzed conditions, **246** was afforded in 29% yield as the minor product through the hydration process due to the modest diastereocontrol. Meanwhile, cedrol (**241**) could be converted to **247** in thirteen steps. A hydration reaction was conducted with a Mn-catalyst to give **248** in 50% yield.

Scheme 30 Maimone's synthesis of *Illicium* sesquiterpenes.

Scheme 31 Ding's synthesis of (+)-sarcophytin (255).

In 2019, Ding and co-workers accomplished the synthesis of cembrane diterpenoids, (+)-sarcophytin (**255**) (Scheme 31).<sup>53</sup> They employed Mukaiyama hydration to introduce the tertiary alcohol. The synthesis commenced with the construction of bicyclic **252**, which was accessed through double-Mukaiyama Michael addition between **250** and the Rawal diene **251** and elimination. **253** was then furnished in three steps from **252**. The authors speculated that the subsequent hydration would take place from the  $\beta$ -face since the proximate pseudoaxial hydroxy group blocks the  $\alpha$ -face. As expected, subjecting **253** to Shenvi's optimized hydration conditions ( $\text{Mn(dpm)}_3$ ,  $\text{Ph(i-PrO)SiH}_2$ ,  $\text{O}_2$ , and  $\text{THF}$ ) formed **254** and its epimer in a 5.6:1 ratio with 80% yield, favouring desired **254**. In comparison, using other hydride sources ( $\text{EtSiH}_3$ ,  $\text{PhSiH}_3$ , and  $\text{NaBH}_4$ ) and metal catalysts ( $\text{Co(acac)}_2$ ,  $\text{Co(tfa)}_2$ ,  $\text{Mn(acac)}_3$ , and  $\text{Fe(acac)}_3$ ) led to inferior yield (15–60%) and diastereoselectivity (1.2:1–4.5:1). Necessary functional group transformations eventually led to (+)-sarcophytin (**255**).

In 2019, Li and co-workers reported the synthesis of arcutinidine, arcutinine, and arcutine. Mukaiyama hydration was adopted (Scheme 32).<sup>54</sup> Alcohol **257** was made from alcohol **256** through sequential intermolecular and anionic Diels–Alder reactions. A dehydration reaction of **257** with  $\text{SOCl}_2$  furnished a trisubstituted olefin which could further be converted to **258** through a Prins/Wagner–Meerwein cascade reaction. Mukaiyama hydration of **258** with  $\text{Mn(acac)}_2$  and  $\text{PhSiH}_3$  furnished tertiary alcohol **259** with the desired stereochemistry after site-selective C–H oxidation. In addition, the authors

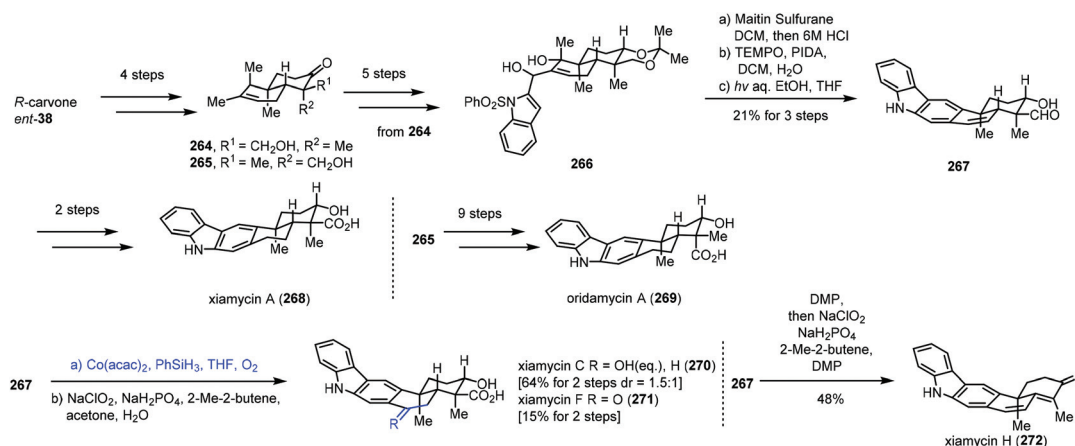


**Scheme 32** Li's synthesis of arcutinidine (261), arcutinine (262) and arcutine (263).

found that Mn(acac)<sub>2</sub> as a precatalyst was superior to Co(acac)<sub>2</sub> for this olefin hydration. Diketoaldehyde 260 was then prepared in five steps. Chemoselective condensation and 1,2-reduction provided the corresponding oxime, followed by cleavage of the N–O bond and reduction giving arcutinidine (261).

Arcutinine (262) and arcutine (263) were afforded from arcutinidine (261) *via* acylation, respectively.

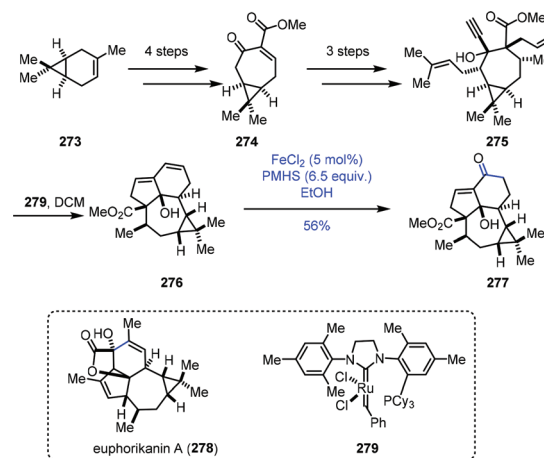
In 2019, Sarpong and co-workers reported total synthesis of xiamycins A (268), C (270), F (271), and H (272) and oridamycin A (269) (Scheme 33).<sup>55</sup> In this case, they employed Mukaiyama hydration to achieve functionalization of endocyclic disubstituted olefins. Their synthesis commenced with the assembly of the *trans*-decalin framework. (*R*)-Carvone was transformed to 264 and 265 in four steps. Diol 266 was furnished from 264. Dehydration of 266, followed by oxidation and key photocyclization–desulfonylation, led to aldehyde 267. Xiamycin A (268) was obtained after two more steps. Subjecting 267 to Mukaiyama hydration conditions (Co(acac)<sub>2</sub>, PhSiH<sub>3</sub>, THF, and O<sub>2</sub>) followed by Pinnick oxidation provided xiamycin C (270) and its C-19 epimer and xiamycin F (271). Meanwhile, xiamycin H (272) was generated from 267 in steps.



**Scheme 33** Sarpong's synthesis of xiamycins A (268), C (270), F (271), and H (272) and oridamycin A (269).

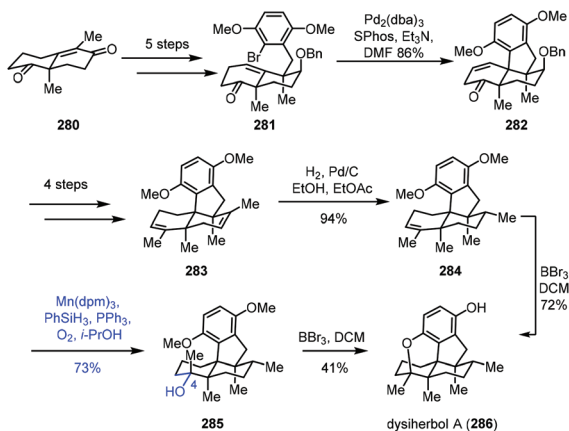
A similar conversion was performed by Yang and co-workers in the synthesis of the core structure of euphorikanin A (Scheme 34).<sup>56</sup> The 7/3-bicyclic 274 was synthesized from (+)-3-carene 273 in four steps. Three more steps of conversions gave the key dienyne precursor 275. A domino RCM reaction of 275 with Grubbs second-generation catalyst 279 proceeded well to deliver the tetracyclic skeleton 276 in excellent yield. To realize the transformation of the conjugated double bonds into the  $\alpha,\beta$ -unsaturated ketone, they tested diene 276 with various Wacker reactions, such as PdCl<sub>2</sub> and CuCl, which led to no reaction, probably due to the high rigidity of the ring system. Then they resorted to HAT-initiated oxidation. Screening of different Fe(II) catalysts, silane reagents, solvents, temperatures and reaction times revealed that FeCl<sub>2</sub>/PMHS/EtOH was optimal, and the desired enone 277 could be obtained successfully in 56% yield.

In 2021, Lu and co-workers described the synthesis of dysiherbol A (286) (Scheme 35).<sup>57</sup> The Wieland–Miescher ketone derivative 280 could be advanced to ketone 281 in five steps. The Pd-catalyzed intramolecular Heck reaction was carried out



**Scheme 34** Yang's synthesis of the core structure of euphorikanin A.



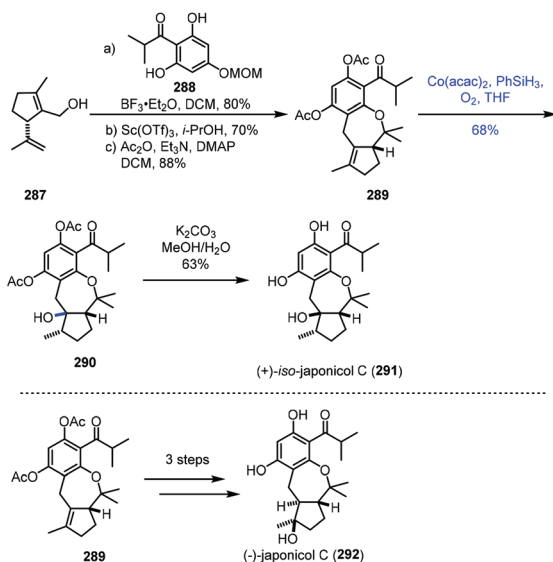


Scheme 35 Lu's synthesis of dysiherbol A (286).

to obtain tetracyclic **282**, which was advanced to diene **283** in four steps. Mono-alkene **284** was created from diene **283** *via* chemo- and diastereoselective reduction. The authors observed that the epoxidation of alkene **284** with  $\text{H}_2\text{O}_2$ , *m*-CPBA, TBHP or  $\text{Vo}(\text{acac})_2$  and TBHP led to the skeleton rearrangement presumably due to the strain of the 6/5-fused ring system. Dihydroxylation of alkene **284** with  $\text{OsO}_4$ ,  $\text{K}_2\text{OsO}_4 \cdot \text{H}_2\text{O}$  or  $\text{AD-mix-}\alpha$  also failed.

Fortunately, Mukaiyama hydration of **284** worked, giving **285** under optimized conditions ( $\text{Mn}(\text{dpm})_3$ ,  $\text{PhSiH}_3$ ,  $\text{O}_2$ , and  $\text{PPh}_3$ ) in 73% yield. They further separated the natural product dysiherbol A (**286**) upon exposure of **285** to  $\text{BBr}_3$ . Monitoring of the reaction revealed that the tertiary alcohol of **285** dehydrated in the presence of  $\text{BBr}_3$  to return to compound **284**. Therefore, **284** was then transformed into dysiherbol A (**286**) directly with  $\text{BBr}_3$ .

In 2021, Dethé and Nirpal disclosed the synthesis of japonicol C (**292**) (Scheme 36).<sup>58</sup> **289** was obtained from **287** through Friedel–Crafts reaction, deprotection and acetylation. The



Scheme 36 Dethé's synthesis of japonicol C (292).

authors then tested the hydration reaction using various metal catalysts. Treatment of **289** with Mn or Fe complexes in the presence of  $\text{PhSiH}_3$  or  $\text{EtSiH}_3$  in solvents like 1,2-dichloroethane, EtOH or *i*-PrOH led to no reaction. Under Mukaiyama hydration conditions,  $\text{Co}(\text{acac})_2$  and phenylsilane in THF under  $\text{O}_2$ , undesired tertiary alcohol **290** was isolated in 68% yield. The authors proposed that the stereochemical outcome of the hydration could be due to the less hindered  $\beta$ -face. Deacetylation of **290** gave **291**, a regioisomer of the natural product japonicol C. Since **290** turned out to be an undesired hydration product, to overcome the regioselectivity issue, the authors attempted Fuch's C–H oxidation method and accessed the desired tertiary alcohol from **289**, which was finally elaborated to japonicol C (**292**).

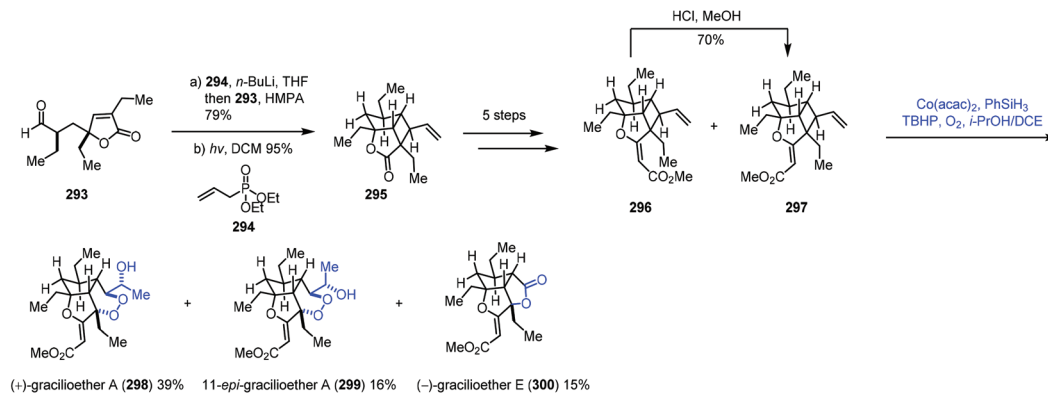
### 3.2 Hydroperoxidation

In this sub-section, we will introduce hydroperoxidation of olefins and its application in natural product synthesis. A number of important works have been summarized in other reviews,<sup>9,10</sup> such as those by Maimone<sup>59</sup> and Inoue.<sup>60</sup> We will focus on the studies published in recent years.

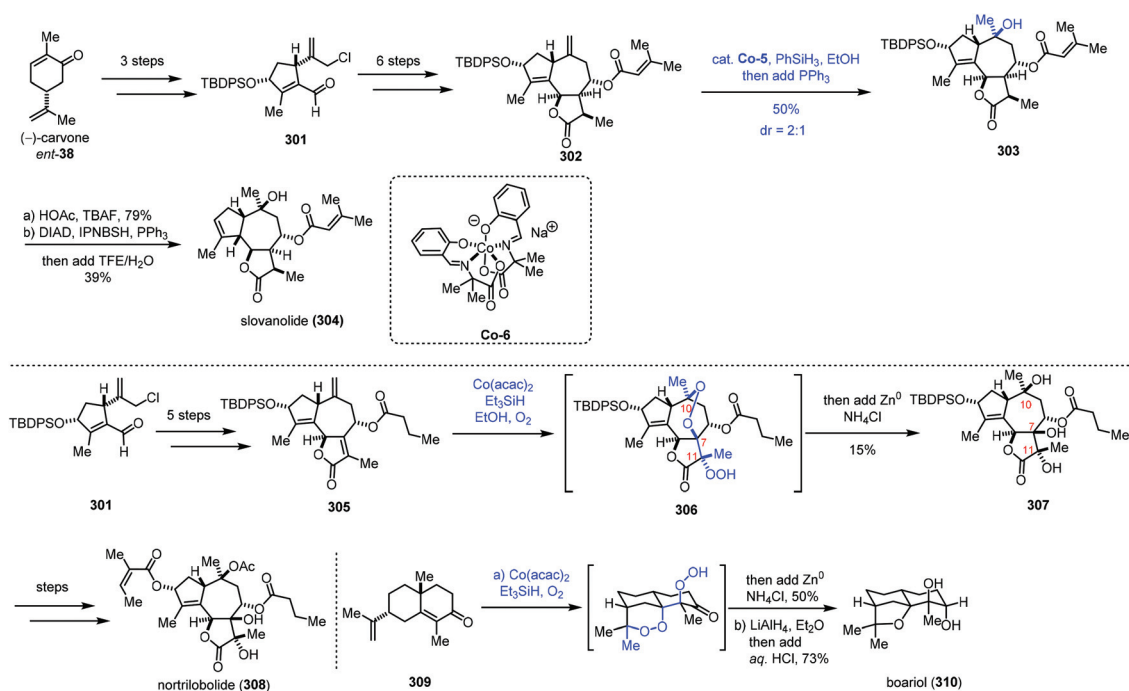
In 2018, Tang and co-workers used the Co-catalyzed HAT to oxygenation of vinylcyclobutane in the syntheses of (+)-gracilioether A (**298**) and (–)-gracilioether E (**300**) (Scheme 37).<sup>61</sup> A Horner–Wadsworth–Emmons reaction of **293** with **294** furnished a diene, which cyclized into vinylcyclobutane **295** through [2 + 2] photocycloaddition, which was advanced to the key compound **297**. They initially tried to construct a six-membered peroxy ring through a radical process as reported by Feldman;<sup>62</sup> however, they failed to get the desired result. Inspired by Maimone's<sup>59</sup> experience in the synthesis of (+)-cardamom peroxide using the Mn-catalyzed HAT to construct a peroxy group, the authors tested Maimone's MHAT conditions ( $\text{Mn}(\text{dpm})_3$ ,  $\text{PhSiH}_3$ , TBHP,  $\text{O}_2$ , and *i*-PrOH/DCM), and only 5% of gracilioether A (**298**) and 7% of gracilioether E (**300**) were isolated. Further optimization revealed that the Mukaiyama/Isayama hydrosilyl peroxidation reaction system was superior ( $\text{Co}(\text{acac})_2$ ,  $\text{PhSiH}_3$ , TBHP,  $\text{O}_2$ , and *i*-PrOH/DCE), and **297** could be converted to gracilioether A (**298**), **299** and gracilioether E (**300**) in acceptable yields. Mechanistically, the authors proposed that the radical is generated from the terminal alkene **297** by HAT from  $\text{HCo}(\text{III})$ , which undergoes cyclobutane ring-opening, dioxygen trapping of the resulting radical, 6-*exo-trig* cyclization, and second dioxygen insertion to give the corresponding peroxy radical. Subsequent hydrogen abstraction and peroxide reduction deliver **298** and **300**.

In 2019, Maimone and co-workers reported the synthesis of complex guaianolide sesquiterpenes (Scheme 38).<sup>63</sup> In the synthesis of nortrilobolide (**308**), they creatively employed the radical tandem reaction under Co-catalyzed HAT conditions to introduce three hydroxyl groups through reduction of the peroxy bond generated.

**301** was prepared from carvone in three steps. Then **301** was converted to the 5,7,5-fused ring system **302** through a six-step sequence. Under MHAT conditions of a Co complex,  $\text{PhSiH}_3$  and  $\text{PPh}_3$  in EtOH, the exocyclic olefin was trans-



**Scheme 37** Tang's synthesis of (+)-gracilioether A (298) and (-)-gracilioether E (300).

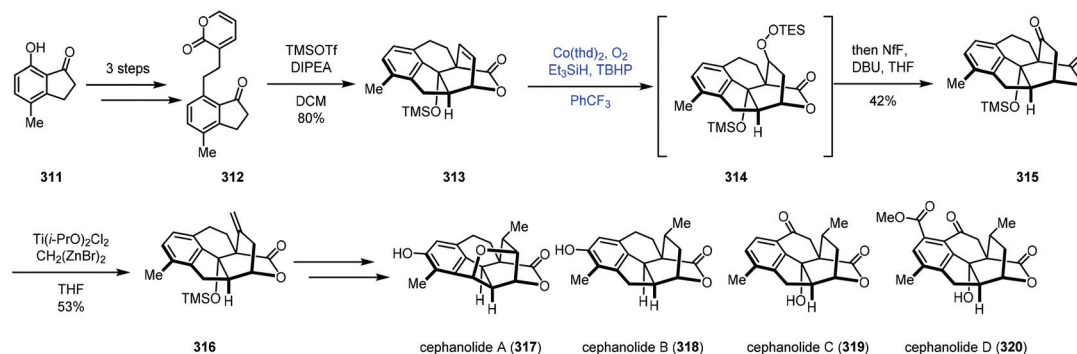


**Scheme 38** Maimone's synthesis of complex guaianolide sesquiterpenes.

formed to the corresponding tertiary alcohol, furnishing **303**. Deprotection and reductive allylic transposition were conducted to give slovanolide (**304**). Regarding the synthesis of heavily oxidized nortrilobolide (**308**), they prepared **305** from **301** at first. Inspired by their synthesis of cardamom peroxide,<sup>59</sup> the authors envisioned that a polyoxygenation cascade with molecular oxygen may be applicable to secure the requisite hydroxyl groups at C10, C7, and C11 of nortrilobolide. Subjecting **305** to Co-catalyzed Mukaiyama hydroperoxidation conditions, followed by reduction with metal Zn provided **307** in 15% yield. Although the yield of the step is low, the cascade process is rather impressive as three hydroxyl groups were installed with the desired configurations in a single operation. The authors noted that any variation of these conditions did not lead to

desired **307**. Based on the experimental results, the authors found that the major side reactions are premature reduction of the first peroxy radical intermediate and formation of an unstable peroxide. Lastly, **307** could be transformed to nortrilobolide (**308**). Maimone and co-workers also completed the synthesis of boariol *via* a similar radical process.

In 2021, Sarpong reported divergent syntheses of cephalanols A–D *via* the common intermediate **316** (Scheme 39).<sup>64</sup> They employed Co-catalyzed radical hydroperoxidation to achieve olefin functionalization. The indanone derivative **312** was created from 7-hydroxy-4-methylindanone (**311**). Exposure of **312** to two equivalents of TMSOTf induced Diels–Alder cycloaddition conditions to provide the core skeleton **313**. Functionalization of the bridging olefin group of **313** proved



Scheme 39 Sarpong's synthesis of cephanolides A–D.

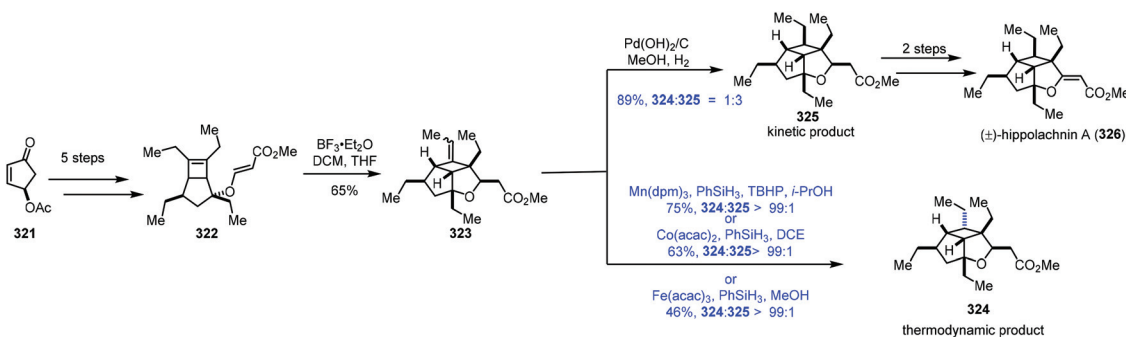
unfruitful. Due to the electron deficiency of olefins, conventional methods such as hydroboration and epoxidation all failed. Thus the authors turned their attention to the MHAT process. A modified Mukaiyama hydration process by Inoue was feasible ( $\text{Co}(\text{thd})_2$ ,  $\text{O}_2$ ,  $\text{Et}_3\text{SiH}$ , and TBHP), giving ketone **315** in 42% yield after treatment of the mixture with DBU. The authors proposed that the regioselectivity of the hydrocobaltation likely correlates with the proximal oxygen lone pair of the lactone. Next, olefination with a combination of  $\text{Ti}(\text{i-PrO})_2\text{Cl}_2$  and Nysted reagent gave **316**, which could be elaborated to cephanolides A–D, respectively.

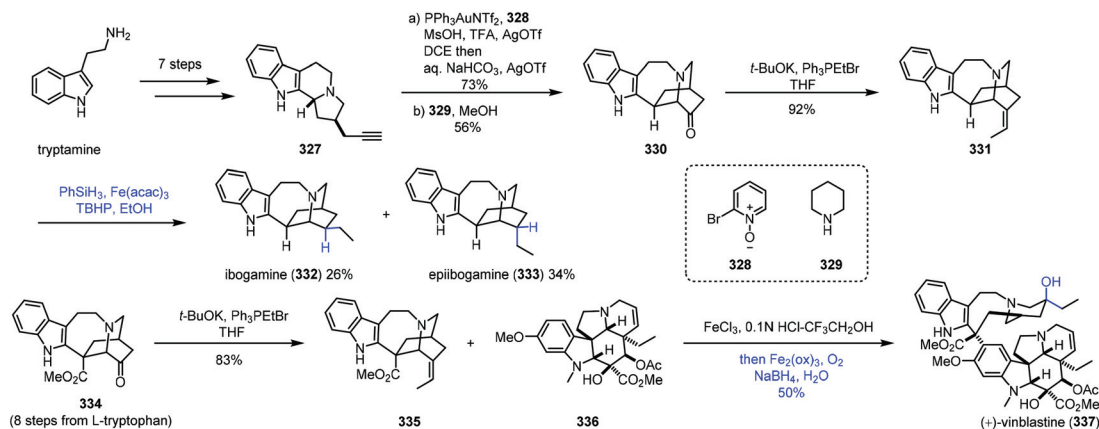
## 4. Hydrogenation

In the process of studying the hydration reaction of olefins with Co catalysts in secondary alcohols in 1989, Mukaiyama noted that the hydrogenation product was obtained as the minor product.<sup>2</sup> In 2000, Magnus discovered that under the conditions of  $\text{Mn}(\text{dpm})_3$ /phenylsilane with the exclusion of air,  $\alpha,\beta$ -unsaturated ketones could be transformed to saturated ketones.<sup>65</sup> In 2014, Shenvi<sup>5a</sup> and Herzon<sup>6</sup> independently reported using MHAT to achieve hydrogenation of unactivated olefins or alkenyl halides, greatly expanding the substrate scope. Since then, hydrogenation of olefins under MHAT conditions has been serving as an alternative to the conventional methods, and has been widely used in organic synthesis.

In their synthesis of hippolachnin A (**326**) in 2015, Carreira tested MHAT-based hydrogenation of exocyclic double bonds (Scheme 40).<sup>66</sup> Cyclopentenone **321** could be transformed to the bicyclic compound **322** via a five-step sequence. An ene cyclization with  $\text{BF}_3 \cdot \text{Et}_2\text{O}$  furnished **323**. When  $\text{Mn}(\text{dpm})_3$  or  $\text{Co}(\text{acac})_2$  or  $\text{Fe}(\text{acac})_3$  was used as the catalyst in the presence of  $\text{PhSiH}_3$ , they found that the undesired thermodynamic product **324** predominated. In contrast, the use of Pearlman's catalyst under a  $\text{H}_2$  atmosphere gave a mixture of the desired kinetic product **325** and **324** (dr = 3 : 1), favouring **325**. Hippolachnin A (**326**) could be obtained from **325** in two steps.

In 2016, Luo and co-workers finished the synthesis of various iboga alkaloids,<sup>67</sup> in which iron-catalyzed HAT was performed to achieve hydrogenation and hydration of alkenes (Scheme 41). Starting from tryptamine, tertiary amine **327** was obtained in seven steps, which could be transformed to **330** via gold-catalyzed oxidation, alkylation and Stevens rearrangement. The Wittig reaction furnished alkene **331**, and the double bond could be reduced to ibogamine (**332**) and epiibogamine (**333**) via Fe-catalyzed HAT-based hydrogenation, slightly preferring undesired **333**. Manganese and cobalt-based catalysts were inferior in this case since **333** was afforded as the predominant product with these catalysts. Moreover, activated Pd/C and  $\text{H}_2$  conditions also gave **333** in high yield. In the synthesis of vinblastine (**337**), the advanced intermediate **334** was furnished from L-tryptophan in eight

Scheme 40 Carreira's synthesis of hippolachnin A (**326**).



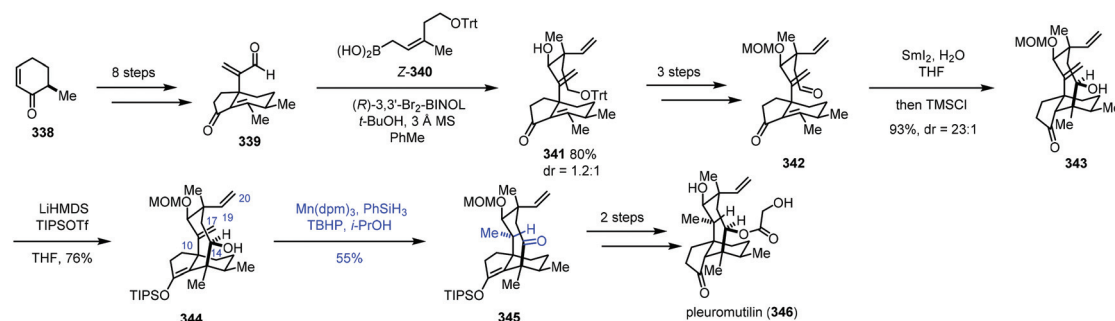
**Scheme 41** Luo's synthesis of various iboga alkaloids.

steps. Wittig reaction of **334** furnished the fragment **335**. Using the conditions reported by Boger and co-workers,<sup>8</sup> Fe(III)-promoted coupling of **335** with the commercially available vindoline **336** gave the coupled product, which was treated with an Fe(III)-NaBH<sub>4</sub>/O<sub>2</sub> solution to selectively hydrate the resulting trisubstituted alkene and reduce the iminium ion, providing vinblastine (**337**) in 50% yield.

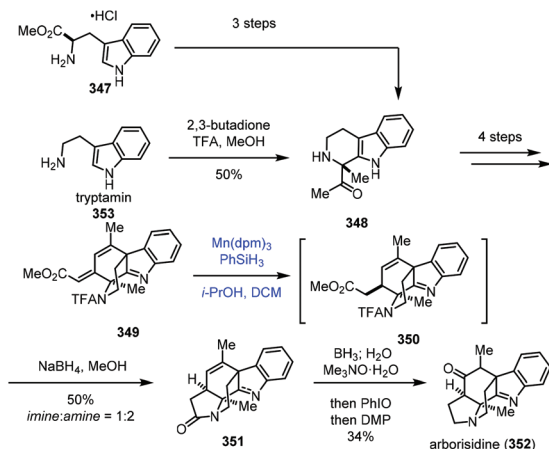
In Reisman's synthesis of pleuromutilin,<sup>68</sup> regarding the HAT-based hydrogenation step, an intramolecular abstraction of protons to rationalize the formation mechanism of the unexpected product **345** was proposed (Scheme 42). Bicycle **339** was synthesized from enone **338** in eight steps. Asymmetric allylboration with *Z*-**340** gave desired **341**, which could be transformed to **342** by a three-step sequence. An eight-membered ring was formed through a SmI<sub>2</sub>-promoted cyclization, delivering tricyclic **343**. Enol ether **344** was then prepared. To finish the synthesis of pleuromutilin, chemo-selective reduction of the C10–C17 exocyclic olefin was required. However, under the standard hydrogenation conditions with a cationic transition metal, hydrogenation of the more accessible C19–C20 vinyl group occurred. Thus the authors turned to MHAT reactions. HAT-type hydrogenation of **344** under the conditions Mn(dpm)<sub>3</sub>/PhSiH<sub>3</sub>/TBHP/*i*-PrOH led to unexpected **345** in 55% yield, in which the C10–C17 olefin was reduced and C14 alcohol was oxidized to ketone. Only trace amounts of products arising from C19–C20 vinyl

reduction were noticed, which is in stark contrast to the standard hydrogenation conditions with a cationic transition metal. The authors thus proposed that a transannular [1,5]-HAT process occurs and cleavage of O–H bonds to form a ketone is a driving force of this conversion. The hypothesis is supported by deuterium-labeling experimental results. Besides, HAT-type hydrogenation of the protected C14 alcohol substrate gave the corresponding C10 alcohol as a mixture of diastereomers with only 6–10% conversion. Finally, pleuromutilin (**346**) was obtained after reduction, acylation and deprotection.

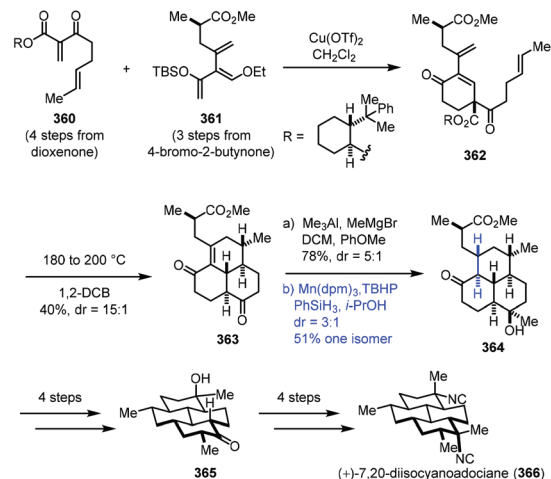
In 2019, Snyder and co-workers reported the synthesis of arborisidine (Scheme 43).<sup>69</sup> They conducted a Mn-catalyzed hydrogenation process to realize the 1,4-reduction of dienolate. In their synthesis, the racemic **348** was obtained from tryptamine (**353**) via Pictet–Spengler reaction, while an enantioselective synthesis of **348** was achieved by a three-step sequence from *D*-tryptophan methyl ester. **348** was then advanced to tetracyclic dienolate **349**. Conventional dienolate hydrogenation and conjugate reduction methods failed with **349**. Under such circumstances, they tried radical hydrogenation conditions with Mn(dpm)<sub>3</sub>/PhSiH<sub>3</sub>, and the desired 1,4-reduction product **350** could be produced. The optimization results showed that the best conversion required using Mn(dpm)<sub>3</sub> in a 50% loading, excess amounts of PhSiH<sub>3</sub> and trace air as the activator of the catalyst. Arborisidine (**352**) was thus



**Scheme 42** Reisman's synthesis of pleuromutilin (**346**).



Scheme 43 Snyder's synthesis of arborisidine (352).



Scheme 45 Shenvi's synthesis of (+)-7,20-diisocyanoadociane (366).

synthesized after lactamization and functional group conversions.

In Yang's synthesis of waihoensene (359) in 2020 (Scheme 44),<sup>70</sup> it is interesting to note that HAT-type hydrogenation gave a higher yield of the desired product with the tetracyclic substrate 357. The tetracyclic substrate 357 was synthesized from enone 354 through Conia-ene type cyclization and Pauson–Khand reaction. Conventional hydrogenation with common metal catalysts led to an undesired diastereomer. HAT-type hydrogenation with Fe(acac)<sub>3</sub> as the catalyst, in contrast, generated desired 358 in 75% yield. The authors envisioned that the resulting C9 radical from 357 would abstract a proton from the proximal C3 next to the C2 carbonyl group through an intramolecular HAT, and the proposed pathway might account for the high diastereoselective reduction. They also conducted a density functional theory (DFT) experiment to further rationalize the observed selectivity. Waihoensene (359) was then furnished *via* methylation and methylenation.

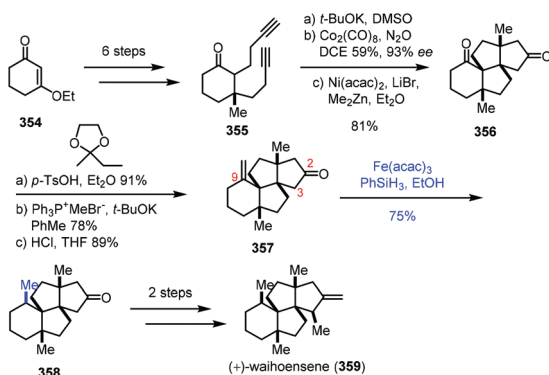
In 2016, Shenvi and co-workers accomplished the synthesis of (+)-7,20-diisocyanoadociane (Scheme 45).<sup>71</sup> They employed Mn-catalyzed radical hydrogenation of a conjugated tetrasubstituted olefin to access the thermodynamic product. Starting materials 360 and 361 were obtained from dioxenone and

4-bromo-2-butyne, respectively. An intermolecular Diels–Alder cycloaddition between 360 and 361 with Cu(OTf)<sub>2</sub> furnished 362, which was transformed to tricyclic 363 by an intramolecular Diels–Alder cycloaddition at 180 °C and removal of the auxiliary at 200 °C. Methylation generated the corresponding alcohol. Upon exposure of the alcohol to a Pd, Pt, or Rh catalyst, undesired deconjugation occurred. They eventually found that the hydrogenation of the highly strained alkene could be realized under MHAT conditions (Mn(dpm)<sub>3</sub>, TBHP, PhSiH<sub>3</sub>, and *i*-PrOH), delivering the thermodynamic product 364 in 51% yield as the major isomer. Tricyclic 364 was advanced to (+)-7,20-diisocyanoadociane (366) in eight steps.

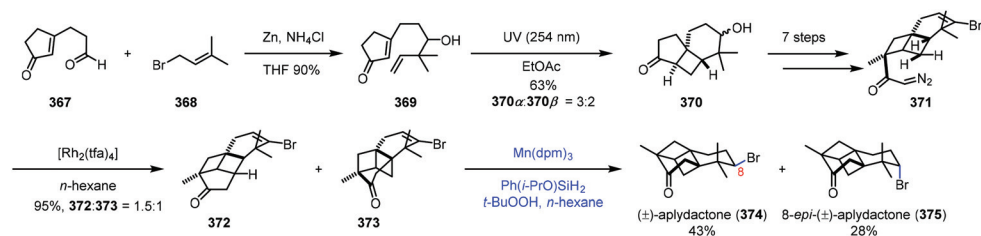
In the synthesis of aplydactone in 2017,<sup>72</sup> Zhang and co-workers employed a strategy to realize hydrogenation of vinyl bromide (Scheme 46). Coupling of 367 and 368 led to 369. Irradiation of 369 afforded tricyclic 370 *via* [2 + 2] photocycloaddition, which was converted to 371 in seven steps. Transannular C–H insertion was performed to form the skeletal structure of aplydactone 373 as the minor product. Traditional hydrogenation conditions with Pd/C or PtO<sub>2</sub> as catalysts under H<sub>2</sub> turned out to be ineffective for the reduction of vinyl bromide of 373. To their delight, subjecting 373 to Shenvi's conditions<sup>5b</sup> afforded uneventfully aplydactone (374) and its C8-epimer 375 in 43 and 28% yield, respectively.

In 2018, Dethle completed the synthesis of (+)-taondiol (381) (Scheme 47).<sup>73</sup> Enone 376 was prepared through ketal protection and Robinson-type annulation. Treatment of 376 with a four-step sequence gave 377. Under MHAT conditions with Mn(dpm)<sub>3</sub> and phenylsilane, hydrogenation of the olefin was achieved to give 378. It should be noted that the usual hydrogenation conditions with Pd/C and H<sub>2</sub> were able to reduce the olefin; however, undesired debenzoylation occurred concomitantly. Moving forward, Friedel–Crafts reaction of 379 and 383 with BF<sub>3</sub>·Et<sub>2</sub>O was carried out to attain pentacyclic 380, which was then advanced to (+)-taondiol (381).

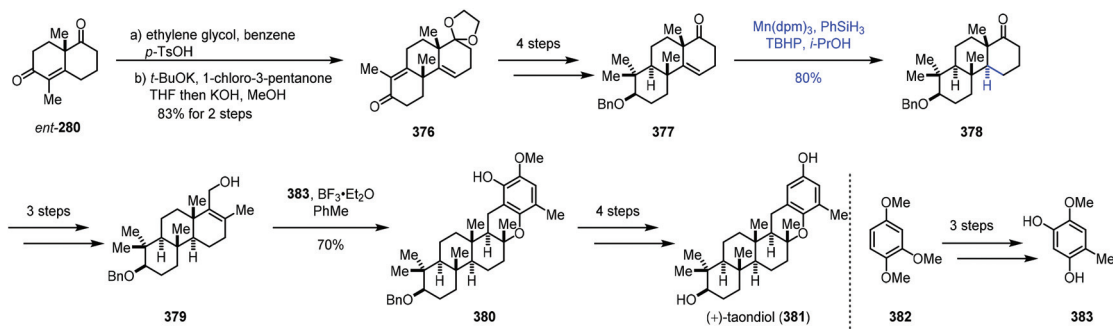
Using the MHAT-based hydrogenation approach, Krische and co-workers completed the synthesis of andrographolide



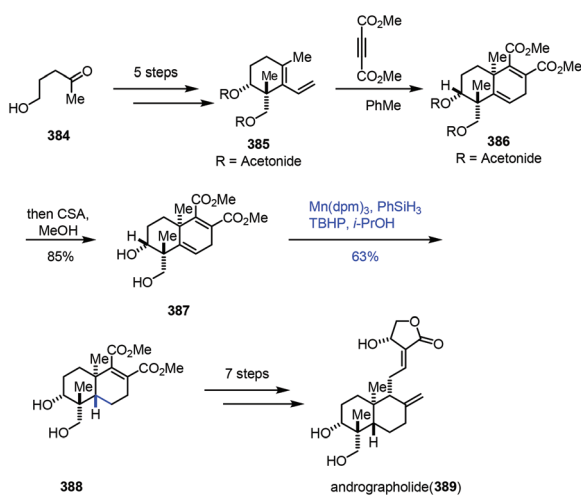
Scheme 44 Yang's synthesis of waihoensene (359).



Scheme 46 Zhang's synthesis of aplydactone (374).



Scheme 47 Dethe's synthesis of (+)-taondioid (381).



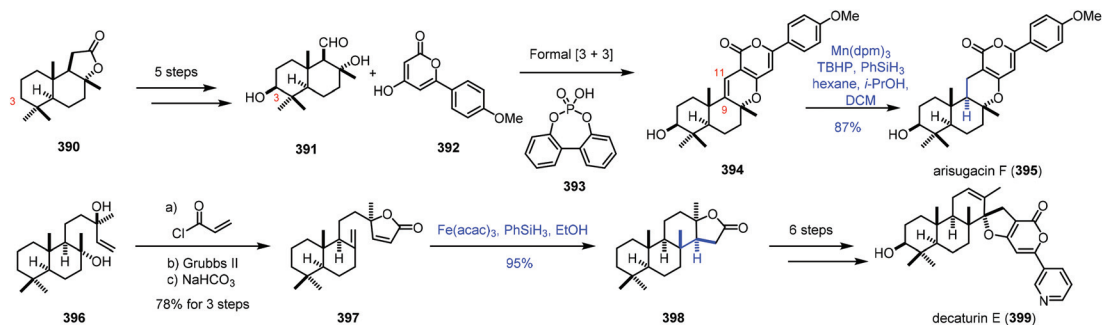
Scheme 48 Krische's synthesis of andrographolide (389).

(Scheme 48).<sup>74</sup> Diene 385 was attained from 5-hydroxy-2-pentanone (384) in five steps. Diels-Alder cycloaddition of diene 385 and dimethyl acetylene dicarboxylate followed by hydrolysis gave diol 387. Chemo- and stereoselective reduction of the alkene was achieved by the Mn-catalyzed hydrogenation reaction in the presence of phenylsilane to give *trans*-decalin 388 in 63% yield. In comparison, a *cis*-decalin product was exclusively formed upon subjecting acetonide 386 to identical reaction conditions. Andrographolide (389) was obtained from 388 in seven steps.

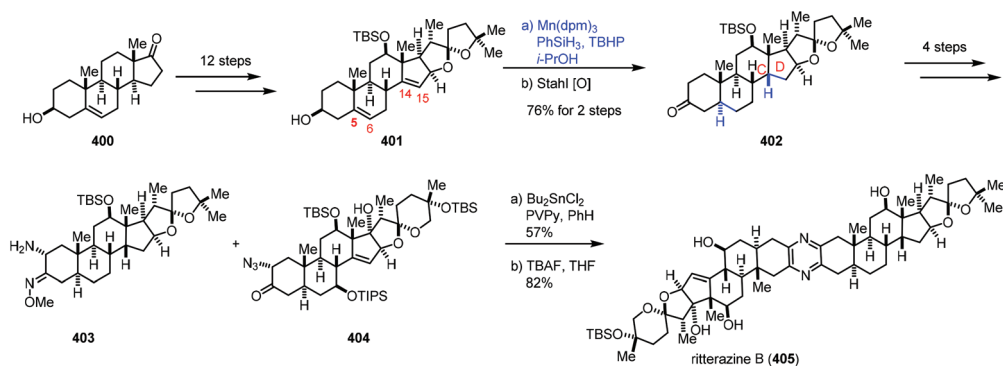
In 2020, Renata and co-workers applied biocatalytic C-H oxidations and MHAT reactions as the main methods to achieve the synthesis of eight meroterpenoid natural products

(Scheme 49).<sup>75</sup> The key common intermediate 391 was obtained from sclareolide 390 by a five-step sequence, featuring biocatalytic C3-hydroxylation. A formal [3 + 3] union of 391 and 392 led to 394. Under the conventional hydrogenation conditions, with Rh, Pt and Pd as catalysts, the reductions occurred at the pyrene moiety. The authors reasoned that MHAT-based reactions would be feasible. The bulky metal catalyst might suppress the reduction of the tetrasubstituted alkene. Among two trisubstituted alkenes, reduction of the C9–C11 alkene would be preferred due to the greater stability of the resulting C9 tertiary radical. Besides, Shenvi discovered that MHAT-based hydrogenation could provide the thermodynamically stable *trans*-decalin product. In practice, the authors discovered that arisugacin F (395) could be accessed by Mn-catalyzed HAT-based hydrogenation (Mn(dpm)<sub>3</sub>, TBHP, and PhSiH<sub>3</sub>) in 87% yield. In addition, HAT-based intramolecular Giese coupling served as the key step in the synthesis of decaturin E (399), in which the *trans*-decalin product 398 was afforded from 397 with complete diastereoselectivity and excellent yield under the conditions of Fe(acac)<sub>3</sub> and PhSiH<sub>3</sub>.

In 2021, Reisman reported the synthesis of ritterazine B (Scheme 50).<sup>76</sup> The advanced diene intermediate 401 was prepared in twelve steps from *trans*-dehydroandrosterone 400. MHAT-based reduction of the C5–C6 and C14–C15 alkenes of 401 proceeded well to give rise to 402 after oxidation. In this case, *cis*-fusion at the C/D ring-junction would be a thermodynamically stable configuration as supported by DFT studies. The authors found that it was difficult to reduce the C14–C15 double bond under conventional hydrogenation conditions. Ritterazine B (405) was accessed by heterodimerization of two advanced fragments 403 and 404 and deprotection.



Scheme 49 Renata's synthesis of oxidized meroterpenoids.



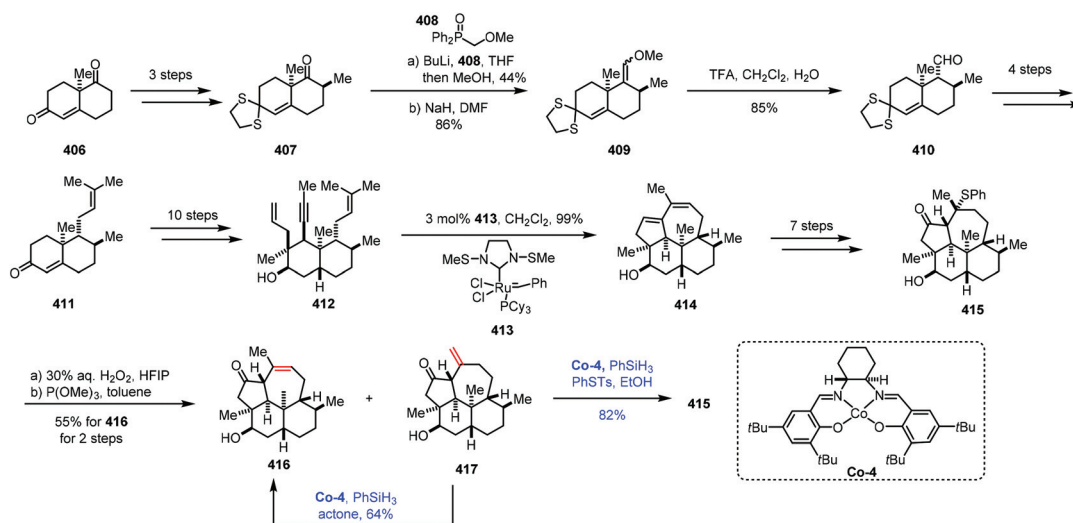
Scheme 50 Reisman's synthesis of oxidized meroterpenoids.

## 5. Isomerization

The isomerization of olefins is a redox neutral process, which could avoid surplus oxidation state manipulation. Mechanistically, the isomerization of olefins mainly proceeds with two different pathways: either a metal hydrogen mechanism or a  $\pi$ -allyl mechanism.<sup>77,78</sup> However, the isomerization of olefins through

MHAT follows a different pathway. In 2014, Holland reported Co-catalyzed isomerization of terminal alkenes to internal *Z*-alkenes *via* most likely the metal hydrogen mechanism.<sup>79</sup> In 2017, Shenvi reported that Co-catalyzed HAT was used to isomerize a terminal alkene to an internal olefin by one position.<sup>5a</sup>

Metz and co-workers subsequently employed Shenvi's method in their synthesis of  $3\beta$ -hydroxy-7 $\beta$ -kemp-8(9)-en-6-one

Scheme 51 Metz's synthesis of  $3\beta$ -hydroxy-7 $\beta$ -kemp-8(9)-en-6-one (416).

(416) in 2017 (Scheme 51).<sup>80</sup> The synthesis commenced with Wieland–Miescher ketone **406**, which was transformed to **407** *via* chemoselective thioetheralization, alkylation and epimerization. The carbonyl group underwent olefination to give compound **409**, followed by acid hydrolysis to lead to **410**. Prenylation provided **411**. A ten-step sequence provided ketone **412**. An olefin metathesis with Grubbs catalyst **413** gave tetracyclic dienol **414**, which could be transformed to **415** *via* a seven-step sequence. Upon treatment of **415** with aqueous hydrogen peroxide followed by heating the resulting mixture, **416** and the exocyclic olefin **417** were isolated. Under the conditions of the cobalt complex **Co-4** and  $\text{PhSiH}_3$ , the exocyclic double bond of **417** could be isomerized to an endocyclic double bond to provide **416** in 64% yield. It should be mentioned that **417** could be used to produce **415** through Co-catalyzed Markovnikov addition of thiophenol.

## 6. Conclusion

The metal-hydride hydrogen atom transfer (MHAT) reaction is a powerful method to functionalize olefins. Here we summarized the applications of MHAT in natural product synthesis. As demonstrated by the aforementioned examples, in many cases, MHAT reactions occur under mild conditions, with high chemoselectivity and high tolerance of functional groups. Besides, Fe, Co, and Mn, the often used metal catalysts in MHAT reactions, are relatively cheap. Based on the aforementioned examples, presumably due to the different reactivities of the metal catalysts, reductive coupling reactions like the Giese reaction and reductive coupling with carbonyl or cyano groups often involve the use of Fe complexes. Hydrogenations use both Mn and Fe metals. With respect to the redox neutral process and hydration and hydroperoxidation reactions, Co and Mn complexes are usually adopted. In particular, Co complexes are the preferred catalysts in hydroarylation and isomerization reactions.

Many reports have shown that C–N or C–X bonds could be formed by MHAT-induced reactions, such as Carreira's hydrohydrazination and Shigehisa's intramolecular hydroamination. However, regarding synthetic applications, there are just limited examples, indicating that in-depth application of these newly developed methods in complex molecule synthesis needs to be exploited in future. Furthermore, a few examples like Liu's synthesis of hispidanin A and Vanderwal's synthesis of plebedipene B have demonstrated the power of MHAT-based polyene cyclization. As such, more sophisticated designs of the MHAT-based cascade strategy in polycyclic or caged architectures, in which multiple bonds could be forged in a single operation, are highly expected.

## Conflicts of interest

There are no conflicts to declare.

## Acknowledgements

We are grateful to the National Natural Science Foundation of China (21871098, 22071064, and 21672073), the National Program on Key Research Project (2016YFA0602900), Guangdong Province Science Foundation (2017B090903003), the Science and Technology Program of Guangzhou (201707010073), and the Fundamental Research Funds for the Central Universities, SCUT for the financial support.

## References

- 1 I. Tabushi and N. Koga, P-450 Type Oxygen Activation by Porphyrin-Manganese Complex, *J. Am. Chem. Soc.*, 1979, **101**, 6456.
- 2 (a) T. Mukaiyama, S. Isayama, S. Inoki, K. Kato, T. Yamada and T. Takai, Oxidation-Reduction Hydration of Olefins with Molecular Oxygen and 2-Propanol Catalyzed by Bis(acetylacetonato)cobalt(II), *Chem. Lett.*, 1989, **18**, 449–452; (b) S. Inoki, K. Kato, T. Takai, S. Isayama, T. Yamada and T. Mukaiyama, Bis(trifluoroacetylacetonato)cobalt(II) Catalyzed Oxidation-Reduction Hydration of Olefins Selective Formation of Alcohols from Olefins, *Chem. Lett.*, 1989, **18**, 515.
- 3 S. Isayama and T. Mukaiyama, Hydration of Olefins with Molecular Oxygen and Triethylsilane Catalyzed by Bis(trifluoroacetylacetonato)cobalt(II), *Chem. Lett.*, 1989, **18**, 569.
- 4 (a) J. Waser and E. M. Carreira, Convenient Synthesis of Alkylhydrazides by the Cobalt-Catalyzed Hydrohydrazination Reaction of Olefins and Azodicarboxylates, *J. Am. Chem. Soc.*, 2004, **126**, 5676; (b) J. Waser and E. M. Carreira, Catalytic Hydrohydrazination of a Wide Range of Alkenes with a Simple Mn Complex, *Angew. Chem., Int. Ed.*, 2004, **43**, 4099; (c) J. Waser, H. Nambu and E. M. Carreira, Cobalt-Catalyzed Hydroazidation of Olefins: Convenient Access to Alkyl Azides, *J. Am. Chem. Soc.*, 2005, **127**, 8294; (d) J. Waser, B. Gaspar, H. Nambu and E. M. Carreira, Hydrazines and Azides via the Metal-Catalyzed Hydrohydrazination and Hydroazidation of Olefins, *J. Am. Chem. Soc.*, 2006, **128**, 11693; (e) B. Gaspar and E. M. Carreira, Mild Cobalt-Catalyzed Hydrocyanation of Olefins with Tosyl Cyanide, *Angew. Chem., Int. Ed.*, 2007, **46**, 4519; (f) B. Gaspar and E. M. Carreira, Catalytic Hydrochlorination of Unactivated Olefins with *para*-Toluenesulfonyl Chloride, *Angew. Chem., Int. Ed.*, 2008, **47**, 5758; (g) B. Gaspar and E. M. Carreira, Cobalt Catalyzed Functionalization of Unactivated Alkenes: Regioselective Reductive C–C Bond Forming Reactions, *J. Am. Chem. Soc.*, 2009, **131**, 13214.
- 5 (a) S. W. M. Crossley, F. Barabé and R. A. Shenvi, Simple, Chemoselective, Catalytic Olefin Isomerization, *J. Am. Chem. Soc.*, 2014, **136**, 16788; (b) K. Iwasaki, K. K. Wan, A. Oppedisano, S. W. M. Crossley and R. A. Shenvi, Simple,



- Chemoselective Hydrogenation with Thermodynamic Stereocontrol, *J. Am. Chem. Soc.*, 2014, **136**, 1300.
- 6 S. M. King, X.-S. Ma and S. B. Herzon, A Method for the Selective Hydrogenation of Alkenyl Halides to Alkyl Halides, *J. Am. Chem. Soc.*, 2014, **136**, 6884.
- 7 (a) J. C. Lo, J.-H. Gui, Y. Yabe, C. M. Pan and P. S. Baran, Functionalized olefin cross-coupling to construct carbon–carbon bonds, *Nature*, 2014, **516**, 343; (b) M. Yan, J. C. Lo, J. T. Edwards and P. S. Baran, Radicals: Reactive Intermediates with Translational Potential, *J. Am. Chem. Soc.*, 2016, **138**, 12692; (c) J. C. Lo, Y. Yabe and P. S. Baran, A Practical and Catalytic Reductive Olefin Coupling, *J. Am. Chem. Soc.*, 2014, **136**, 1304.
- 8 (a) H. Ishikawa, D. A. Colby, S. Seto, P. Va, A. Tam, H. Kakei, T. J. Rayl, I. Hwang and D. L. Boger, Total Synthesis of Vinblastine, Vincristine, Related Natural Products, and Key Structural Analogues, *J. Am. Chem. Soc.*, 2009, **131**, 4904; (b) J. E. Sears and D. L. Boger, Total Synthesis of Vinblastine, Related Natural Products, and Key Analogues and Development of Inspired Methodology Suitable for the Systematic Study of Their Structure–Function Properties, *Acc. Chem. Res.*, 2015, **48**, 653.
- 9 (a) S. W. M. Crossley, C. Obradors, R. M. Martinez and R. A. Shenvi, Mn-, Fe-, and Co-Catalyzed Radical Hydrofunctionalizations of Olefins, *Chem. Rev.*, 2016, **116**, 8912; (b) S. A. Green, S. W. M. Crossley, J. L. M. Matos, S. Vasquez-Cespedes, S. L. Shevick and R. A. Shenvi, The High Chemofidelity of Metal-Catalyzed Hydrogen Atom Transfer, *Acc. Chem. Res.*, 2018, **51**, 2628.
- 10 (a) S. H. Gao and Y. Y. Qiu, Advances of Radical and Photo Reactions in Natural Products Synthesis, *Sci. China: Chem.*, 2016, **59**, 1093; (b) M. Yan, J. C. Lo, J. T. Edwards and P. S. Baran, Radicals: Reactive Intermediates with Translational Potential, *J. Am. Chem. Soc.*, 2016, **138**, 12692; (c) J. E. Zweig, D. E. Kim and T. R. Newhouse, Methods Utilizing First-Row Transition Metals in Natural Product Total Synthesis, *Chem. Rev.*, 2017, **117**, 11680; (d) S. L. Shevick, C. V. Wilson, S. Kotesova, D. Kim, P. L. Holland and R. A. Shenvi, Catalytic Hydrogen Atom Transfer to Alkenes: A Roadmap for Metal Hydrides and Radicals, *Chem. Sci.*, 2020, **11**, 12401; (e) A. Simonneau and M. Oestreich, Fascinating Hydrogen Atom Transfer Chemistry of Alkenes Inspired by Problems in Total Synthesis, *Angew. Chem., Int. Ed.*, 2015, **54**, 3556.
- 11 B. Giese and J. Meister, Die Addition von Kohlenwasserstoffen an Olefine Eine neue synthetische Methode, *Chem. Ber.*, 1977, **110**, 2588.
- 12 T. Taniguchi, N. Goto, A. Nishibata and H. Ishibashi, Iron-Catalyzed Redox Radical Cyclizations of 1,6-Dienes and Enynes, *Org. Lett.*, 2010, **12**, 112.
- 13 D. T. George, E. J. Kuenstner and S. V. Pronin, A Concise Approach to Paxilline Indole Diterpenes, *J. Am. Chem. Soc.*, 2015, **137**, 15410.
- 14 G. Xu, M. Elkin, D. J. Tantillo, T. R. Newhouse and T. J. Maimone, Traversing Biosynthetic Carbocation Landscapes in the Total Synthesis of Andrastin and Terretonin Meroterpenes, *Angew. Chem., Int. Ed.*, 2017, **56**, 12498.
- 15 C. P. Ting, G. Xu, X. Zeng and T. J. Maimone, Annulative Methods Enable a Total Synthesis of the Complex Meroterpene Berkeleyone A, *J. Am. Chem. Soc.*, 2016, **138**, 14868.
- 16 H. Shigehisa, T. Aoki, S. Yamaguchi, N. Shimizu and K. Hiroya, Hydroalkoxylation of Unactivated Olefins with Carbon Radicals and Carbocation Species as Key Intermediates, *J. Am. Chem. Soc.*, 2013, **135**, 10306.
- 17 T. Amatov, R. Pohl, I. Cisařová and U. Jahn, Sequential Oxidative and Reductive Radical Cyclization Approach toward Asperparaline C and Synthesis of Its 8-Oxo Analogue, *Org. Lett.*, 2017, **19**, 1152.
- 18 Z. H. Lu, X. Zhang, Z. C. Guo, Y. Chen, T. Mu and A. Li, Total Synthesis of Aplysiasecosterol A, *J. Am. Chem. Soc.*, 2018, **140**, 9211.
- 19 P. F. Hu, H. M. Chi, K. C. DeBacker, X. Gong, J. H. Keim, I. T. Hsu and S. A. Snyder, Quaternary-Centre-Guided Synthesis of Complex Polycyclic Terpenes, *Nature*, 2019, **569**, 703.
- 20 G. Xu, J. Wu, L. Li, Y. Lu and C. Li, Total Synthesis of (–)-Daphnezomines A and B, *J. Am. Chem. Soc.*, 2020, **142**, 15240.
- 21 X. H. Zeng, V. Shukla and D. L. Boger, Divergent Total Syntheses of (–)-Pseudocopsinine and (–)-Minovincinine, *J. Org. Chem.*, 2020, **85**, 14817.
- 22 P. Q. Chen, C. Wang, R. Yang, H. J. Xu, J. H. Wu, H. F. Jiang, K. Chen and Z. Q. Ma, Asymmetric Total Synthesis of Dankasterones A and B and Periconiastone A through Radical Cyclization, *Angew. Chem., Int. Ed.*, 2021, **60**, 5512.
- 23 Y. Hu, M. Bai, Y. Yang, J. Y. Tian and Q. H. Zhou, Rapid Access to Tetracyclic Core of Wortmannin via an Intramolecular Reductive Olefin Coupling Strategy, *Org. Lett.*, 2020, **22**, 6308.
- 24 H. P. Deng, W. Cao, R. Liu, Y. H. Zhang and B. Liu, Asymmetric Total Synthesis of Hispidanin A, *Angew. Chem., Int. Ed.*, 2017, **56**, 5849.
- 25 W. Cao, H. P. Deng, Y. Sun, B. Liu and S. Qin, Asymmetric Synthesis of Hispidanin A and Related Diterpenoids, *Chem. – Eur. J.*, 2018, **24**, 9120.
- 26 H. M. Boehm, S. Handa, G. Pattenden, L. Roberts, A. J. Blake and W. S. Li, Cascade Radical Cyclisations Leading to Steroid Ring Constructions. Regio- and Stereochemical Studies Using Ester- and Fluoro-Alkene Substituted Polyene Acyl Radical Intermediates, *J. Chem. Soc., Perkin Trans. 1*, 2000, 3522.
- 27 K. Yu, F. Yao, Q. Zeng, H. Xie and H. Ding, Asymmetric Total Syntheses of (+)-Davisinol and (+)-18-Benzoyldavisinol: A HAT-Initiated Transannular Redox Radical Approach, *J. Am. Chem. Soc.*, 2021, **143**, 10576.
- 28 W. P. Thomas, D. J. Schatz, D. T. George and S. V. Pronin, A Radical-Polar Crossover Annulation to Access Terpenoid Motifs, *J. Am. Chem. Soc.*, 2019, **141**, 12246.

- 29 J. R. Andreatta, B. A. McKeown and T. B. Gunnoe, Transition Metal Catalyzed Hydroarylation of Olefins Using Unactivated Substrates: Recent Developments and Challenges, *J. Organomet. Chem.*, 2011, **696**, 305.
- 30 Z. Dong, Z. Ren, S. J. Thompson, Y. Xu and G. Dong, Transition-Metal-Catalyzed C–H Alkylation Using Alkenes, *Chem. Rev.*, 2017, **117**, 9333.
- 31 Y. Ji, Z. Y. Xin, H.-B. He and S. H. Gao, Total Synthesis of Viridin and Viridiol, *J. Am. Chem. Soc.*, 2019, **141**, 16208.
- 32 Z. Y. Xin, H. Wang, H. B. He, X. L. Zhao and S. H. Gao, Asymmetric Total Synthesis of Norzoanthamine, *Angew. Chem., Int. Ed.*, 2021, **60**, 12807.
- 33 B. X. Zhang, W. F. Zheng, X. Q. Wang, D. Q. Sun and C. Z. Li, Total Synthesis of Notoamides F, I, and R and Sclerotiamide, *Angew. Chem., Int. Ed.*, 2016, **55**, 10435.
- 34 D. Vrubliauskas, B. M. Gross and C. D. Vanderwal, Stereocontrolled Radical Bicyclizations of Oxygenated Precursors Enable Short Syntheses of Oxidized Abietane Diterpenoids, *J. Am. Chem. Soc.*, 2021, **143**, 2944.
- 35 (a) H. Y. Jang and M. J. Krische, Catalytic C-C Bond Formation via Capture of Hydrogenation Intermediates, *Acc. Chem. Res.*, 2004, **37**, 653; (b) S. Isayama and T. Mukaiyama, Cobalt(II) Catalyzed Coupling Reaction of  $\alpha,\beta$ -Unsaturated Compounds with Aldehydes by the Use of Phenylsilane. New Method for Preparation of  $\beta$ -Hydroxy Nitriles, Amides, and Esters, *Chem. Lett.*, 1989, **18**, 2005.
- 36 (a) M. Saladrigas, C. Bosch, G. V. Saborit, J. Bonjoch and B. Bradshaw, Radical Cyclization of Alkene-Tethered Ketones Initiated by Hydrogen-Atom Transfer, *Angew. Chem., Int. Ed.*, 2018, **57**, 182; (b) O. J. Turner, J. A. Murphy, D. J. Hirst and E. Talbot, Hydrogen Atom Transfer-Mediated Cyclisations of Nitriles, *Chem. – Eur. J.*, 2018, **24**, 18658.
- 37 G. G. Liu, Z. J. Zhang, S. M. Fu and B. Liu, Asymmetric Total Synthesis of Rumphellclove E, *Org. Lett.*, 2021, **23**, 290.
- 38 J. Liu and D. Ma, A Unified Approach for the Assembly of Atisine- and Hetidine-type Diterpenoid Alkaloids: Total Syntheses of Azitine and the Proposed Structure of Navirine C, *Angew. Chem., Int. Ed.*, 2018, **57**, 6676.
- 39 B. Xu, W. Xun, S.-B. Su and H. B. Zhai, Total Syntheses of (–)-Conidiogenone B, (–)-Conidiogenone, and (–)-Conidiogenol, *Angew. Chem., Int. Ed.*, 2020, **59**, 16475.
- 40 M. Tanaka, C. Mukaiyama, H. Mitsuhashi, M. Maruno and T. Wakamatsu, Synthesis of Optically Pure Gomisi Lignans: The Total Synthesis of (+)-Schizandrin, (+)-Gomisin A, and (+)-Isoschizandrin in Naturally Occurring Forms, *J. Org. Chem.*, 1995, **60**, 4339.
- 41 Y. Matsushita, K. Sugamoto, T. Nakama, T. Sakamoto, T. Matsui and M. Nakayama,  $\gamma$ -Selective Hydroxylation of  $\alpha,\beta,\gamma,\delta$ -Unsaturated Carbonyl Compounds and Its Application to Syntheses of ( $\pm$ )-6-Hydroxyshogaol and Related Furanoids, *Tetrahedron Lett.*, 1995, **36**, 1879.
- 42 H. C. Liu, X. W. Zhang, D. Shan, M. Pitchakuntla, Y. F. Ma and Y. X. Jia, Total Syntheses of Festuclavine, Pyroclavine, Costaclavine, *epi*-Costaclavine, Pibocin A, 9-Deacetoxyfumigaclavine C, Fumigaclavine G, and Dihydrosetoclavine, *Org. Lett.*, 2017, **19**, 3323.
- 43 S. A. Liu and D. Trauner, Asymmetric Synthesis of the Antiviral Diterpene Wickerol A, *J. Am. Chem. Soc.*, 2017, **139**, 9491.
- 44 S. Y. Pan, S. Chen and G. B. Dong, Divergent Total Syntheses of Enmein-Type Natural Products: (–)-Enmein, (–)-Isodocarpin, and (–)-Sculponin R, *Angew. Chem., Int. Ed.*, 2018, **57**, 6333.
- 45 M. J. Cheng, L. P. Zhong, C. C. Gu, X. J. Zhu, B. Chen, J. S. Liu, L. Wang, W. C. Ye and C. C. Li, Asymmetric Total Synthesis of Bufospirostenin A, *J. Am. Chem. Soc.*, 2020, **142**, 12602.
- 46 S. W. M. Crossley, G. H. Tong, M. J. Lambrecht, H. E. Burdge and R. A. Shenvi, Synthesis of (–)-Picrotoxinin by Late-Stage Strong Bond Activation, *J. Am. Chem. Soc.*, 2020, **142**, 11376.
- 47 T. K. Allred, A. P. Dieskau, P. Zhao, G. L. Lackner and L. E. Overman, Enantioselective Total Synthesis of Macfarlandin C, a Spongian Diterpenoid Harboring a Concave-Substituted *cis*-Dioxabicyclo-[3.3.0]octanone Fragment, *Angew. Chem., Int. Ed.*, 2020, **59**, 6268.
- 48 C. Obradors, R. M. Martinez and R. A. Shenvi, Ph(*i*-PrO) SiH<sub>2</sub>: An Exceptional Reductant for Metal-Catalyzed Hydrogen Atom Transfers, *J. Am. Chem. Soc.*, 2016, **138**, 4962.
- 49 M. Ohtawa, M. J. Krambis, R. Cerne, J. M. Schkeryantz, J. M. Witkin and R. A. Shenvi, Synthesis of (–)-11-O-Debenzoyltashironin: Neurotrophic Sesquiterpenes Cause Hyperexcitation, *J. Am. Chem. Soc.*, 2017, **139**, 9637.
- 50 X. H. Zhao, Q. Zhang, J. Y. Du, X. Y. Lu, Y. X. Cao, Y. H. Deng and C. A. Fan, Total Synthesis of ( $\pm$ )-Lycojaponicum D and Lycodoline-Type Lycopodium Alkaloids, *J. Am. Chem. Soc.*, 2017, **139**, 7095.
- 51 (a) A. Baker, R. M. Demoret, M. Ohtawa and R. A. Shenvi, Concise Asymmetric Synthesis of (–)-Bilobalide, *Nature*, 2019, **575**, 643; (b) R. M. Demoret, M. A. Baker, M. Ohtawa, S.-M. Chen, C. C. Lam, S. Khom, M. Roberto, S. Forli, K. N. Houk and R. A. Shenvi, Synthetic, Mechanistic, and Biological Interrogation of *Ginkgobiloba* Chemical Space En Route to (–)-Bilobalide, *J. Am. Chem. Soc.*, 2020, **142**, 18599.
- 52 K. Hung, M. L. Condakes, L. F. T. Novaes, S. J. Harwood, T. Morikawa, Z. Yang and T. J. Maimone, Development of a Terpene Feedstock-Based Oxidative Synthetic Approach to the *Illicium* Sesquiterpenes, *J. Am. Chem. Soc.*, 2019, **141**, 3083.
- 53 C. He, J. Xuan, P. R. Rao, P. P. Xie, X. Hong, X. F. Lin and H. F. Ding, Total Syntheses of (+)-Sarcophytin, (+)-Chatancin, (–)-3-Oxochatancin, and (–)-Pavidolide B: A Divergent Approach, *Angew. Chem., Int. Ed.*, 2019, **58**, 5100.
- 54 S. P. Zhou, K. F. Xia, X. B. Leng and A. Li, Asymmetric Total Synthesis of Arcutinidine, Arcutinine, and Arcutine, *J. Am. Chem. Soc.*, 2019, **141**, 13718.
- 55 M. Pfaffenbach, I. Bakanas, N. R. O'Connor, J. L. Herrick and R. Sarpong, Total Syntheses of Xiamycins A, C, F, H and Oridamycin A and Preliminary Evaluation of their

- Anti-Fungal Properties, *Angew. Chem., Int. Ed.*, 2019, **58**, 15304.
- 56 L. L. Shi, Y. D. He, J. X. Gong and Z. Yang, Concise Gram-Scale Synthesis of Euphorikanin a Skeleton through A Domino Ring-Closing Metathesis Strategy, *Chem. Commun.*, 2020, **56**, 531.
- 57 C. K. Chong, Q. L. Zhang, J. Ke, H. M. Zhang, X. D. Yang, B. J. Wang, W. Ding and Z. Y. Lu, Total Synthesis of Anti-Cancer Meroterpenoids Dysideanone B and Dysiherbol A and Structural Reassignment of Dysiherbol A, *Angew. Chem., Int. Ed.*, 2021, **60**, 13807.
- 58 D. H. Dethe and A. K. Nirpal, Enantiospecific Total Synthesis of (–)-Japonicol C, *Org. Lett.*, 2021, **23**, 2648.
- 59 X. Hu and T. J. Maimone, Four-Step Synthesis of the Antimalarial Cardamom Peroxide via an Oxygen Stitching Strategy, *J. Am. Chem. Soc.*, 2014, **136**, 5287.
- 60 M. Nagatomo, M. Koshimizu, K. Masuda, T. Tabuchi, D. Urabe and M. Inoue, Total Synthesis of Ryanodol, *J. Am. Chem. Soc.*, 2014, **136**, 5916.
- 61 Q. K. Zhao, A. Peuronen, K. Rissanen, D. Enders and Y. F. Tang, Enantioselective Total Syntheses of (+)-Hippolachnin A, (+)-Gracilioether A, (–)-Gracilioether E, and (–)-Gracilioether F, *J. Am. Chem. Soc.*, 2018, **140**, 1937.
- 62 (a) K. S. Feldman and M. Parvez, Synthesis of Polyoxygenated Hydrocarbons via Radical-Mediated Oxygenation of Vinylcyclopropanes, *J. Am. Chem. Soc.*, 1986, **108**, 1328; (b) K. S. Feldman and R. E. Simpson, Oxygenation of Substituted Vinylcyclopropanes: Preparative and Mechanistic Studies, *J. Am. Chem. Soc.*, 1989, **111**, 4878; (c) K. S. Feldman and C. M. Kraebel, Vinylcyclopropane Oxygenation. Anti Diastereoselectivity through an Unexpected Transition-State Geometry, *J. Org. Chem.*, 1992, **57**, 4574.
- 63 X. Hu, A. J. Musacchio, X. Shen, Y. Tao and T. J. Maimone, Allylative Approaches to the Synthesis of Complex Guaianolide Sesquiterpenes from Apiaceae and Asteraceae, *J. Am. Chem. Soc.*, 2019, **141**, 14904.
- 64 M. Haider, G. Sennari, A. Eggert and R. Sarpong, Total Synthesis of the Cephalotaxus Norditerpenoids (±)-Cephanolides A–D, *J. Am. Chem. Soc.*, 2021, **143**, 2710.
- 65 P. Magnus, A. H. Payne, M. J. Waring, D. A. Scott and V. Lynch, Conversion of  $\alpha,\beta$ -Unsaturated Ketones into  $\alpha$ -Hydroxy Ketones Using an Mn<sup>III</sup> Catalyst, Phenylsilane and Dioxigen: Acceleration of Conjugate Hydride Reduction by Dioxigen, *Tetrahedron Lett.*, 2000, **41**, 9725.
- 66 S. A. Ruider, T. Sandmeier and E. M. Carreira, Total Synthesis of (±)-Hippolachnin A, *Angew. Chem., Int. Ed.*, 2015, **54**, 2378.
- 67 Y. Zhang, Y. Xue, G. Li, H. Yuan and T. Luo, Enantioselective Synthesis of *Iboga*, Alkaloids and Vinblastine via Rearrangements of Quaternary Ammoniums, *Chem. Sci.*, 2016, **7**, 5530.
- 68 E. P. Farney, S. S. Feng, F. Schafers and S. E. Reisman, Total Synthesis of (+)-Pleuromutilin, *J. Am. Chem. Soc.*, 2018, **140**, 1267.
- 69 Z. Y. Zhou, A. X. Gao and S. A. Snyder, Total Synthesis of (+)-Arborisidine, *J. Am. Chem. Soc.*, 2019, **141**, 7715.
- 70 Y. Z. Qu, Z. Y. Wang, Z. C. Zhang, W. D. Zhang, J. Huang and Z. Yang, Asymmetric Total Synthesis of (+)-Waihoensene, *J. Am. Chem. Soc.*, 2020, **142**, 6511.
- 71 H. H. Lu, S. V. Pronin, Y. Antonova-Koch, S. Meister, E. A. Winzeler and R. A. Shenvi, Synthesis of (+)-7,20-Diisocyanoadociane and Liver-Stage Antiplasmodial Activity of the Isocyanoterpene Class, *J. Am. Chem. Soc.*, 2016, **138**, 7268.
- 72 C. G. Liu, R. Z. Chen, Y. Shen, Z. H. Liang, Y. H. Hua and Y. D. Zhang, Total Synthesis of Aplydactone by a Conformationally Controlled C–H Functionalization, *Angew. Chem., Int. Ed.*, 2017, **56**, 8187.
- 73 D. H. Dethe, S. Mahapatra and S. K. Sau, Enantioselective Total Synthesis and Assignment of the Absolute Configuration of the Meroterpenoid (+)-Taondiol, *Org. Lett.*, 2018, **20**, 2766.
- 74 L. Yang, T. Wurm, B. S. Poudel and M. J. Krische, Enantioselective Total Synthesis of Andrographolide and 14-Hydroxy-Colladonin: Carbonyl Reductive Coupling and trans-Decalin Formation by Hydrogen Transfer, *Angew. Chem., Int. Ed.*, 2020, **59**, 23169.
- 75 J. Li, F. Z. Li, E. King-Smith and H. Renata, Merging Chemoenzymatic and Radical-Based Retrosynthetic Logic for Rapid and Modular Synthesis of Oxidized Meroterpenoids, *Nat. Chem.*, 2020, **12**, 173.
- 76 Y. Nakayama, M. R. Maser, T. Okita, A. V. Dubrovskiy, T. L. Campbell and S. E. Reisman, Total Synthesis of Ritterazine B, *J. Am. Chem. Soc.*, 2021, **143**, 4187.
- 77 B. M. Trost, Atom Economy-A Challenge for Organic Synthesis: Homogeneous Catalysis Leads the Way, *Angew. Chem., Int. Ed. Engl.*, 1995, **34**, 259.
- 78 E. Larionov, H.-H. Lia and C. Mazet, Well-Defined Transition Metal Hydrides in Catalytic Isomerizations, *Chem. Commun.*, 2014, **50**, 9816.
- 79 C. Chen, T. R. Dugan, W. W. Brennessel, D. J. Weix and P. L. Holland, Z-Selective Alkene Isomerization by High-Spin Cobalt(II) Complexes, *J. Am. Chem. Soc.*, 2014, **136**, 945.
- 80 Y. Wang, A. Jager, M. Gruner, T. Lubken and P. Metz, Enantioselective Total Synthesis of 3b-Hydroxy-7b-kemp-8(9)-en-6-one, a Diterpene Isolated from Higher Termites, *Angew. Chem., Int. Ed.*, 2017, **56**, 15861.